Detectors in Nuclear and Particle Physics

Prof. Dr. Johanna Stachel

Department of Physics und Astronomy
University of Heidelberg

July 17, 2018

10. Detection of neutral particles

modification of similar chapter from H.C. Schultz-Coulon

10.1 Introduction

Electrically neutral particles do not interact via electromagnetic forces; for detection they are thus generally converted into charged particles.

Apart from the converting material, detectors for neutrals use essentially same techniques as those for charged particles.

Examples:

photons: total energy deposited in electromagnetic shower
use energy measurement, shower shape
and information on neutrality (e.g. no track)

neutrons: energy in calorimeter (high energy) or material with large neutron absorption
cross section, such as Li, B, ^{3}He (low energy)
and information on neutrality (e.g. no track)

K_0, Λ, . . .   reconstruction of invariant masses

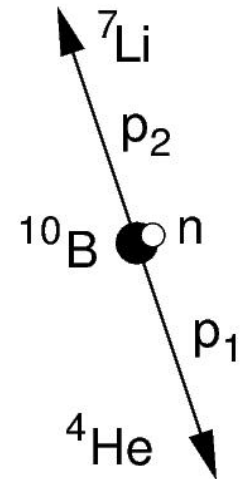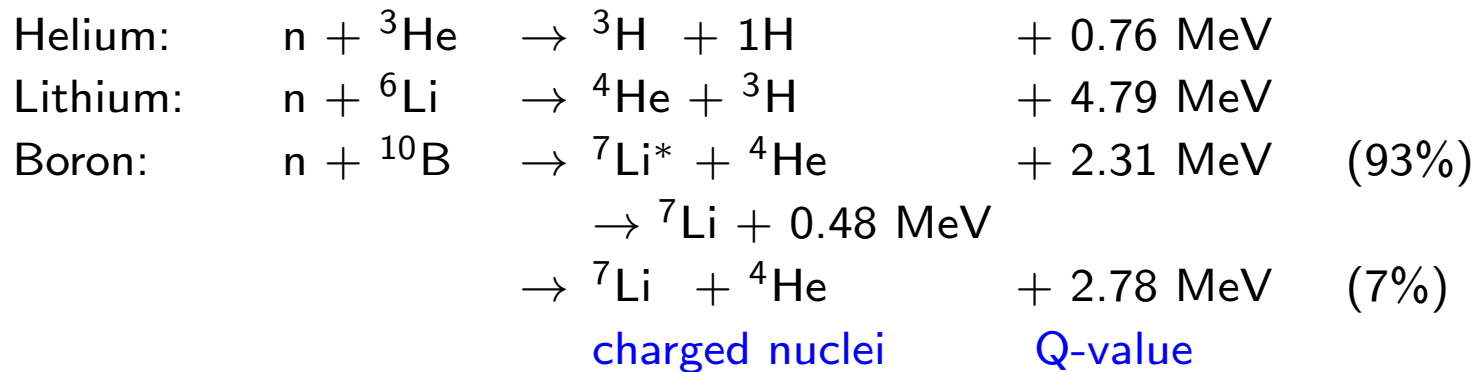neutrinos: identify products of charged and neutral current interactions

10.2 Detection of Neutrons

Neutron detection via nuclear interaction, interaction used varies with the neutron energy:

high energy   hadron calorimeter (see above)

measure energy deposited in form of hadronic shower
neutrality of incident particle has no effect on shower process

moderate energy np-scattering

detection of neutrons by scattering them from material containing
appreciable amounts of hydrogen; recoiling proton is detected

low energy   exothermal nuclear processes

use converter medium with large capture cross-section for slow neutrons;
capture process results in unstable nuclei
subsequent decay products give a detectable signal

Detection of Neutrons

Nuclear reactions used for neutron detectors:

Helium:	$n + {}^3\text{He}$	$\rightarrow {}^3\text{H} + 1\text{H}$	$+ 0.76$ MeV	
Lithium:	$n + {}^6\text{Li}$	$\rightarrow {}^4\text{He} + {}^3\text{H}$	$+ 4.79$ MeV	
Boron:	$n + {}^{10}\text{B}$	$\rightarrow {}^7\text{Li}^* + {}^4\text{He}$	$+ 2.31$ MeV	(93%)
		$\rightarrow {}^7\text{Li} + 0.48$ MeV		
		$\rightarrow {}^7\text{Li} + {}^4\text{He}$	$+ 2.78$ MeV	(7%)

charged nuclei   Q-value

$$\vec{p}_1 = -\vec{p}_2 \qquad\qquad T({}^4\text{He}) = \frac{m_{\text{Li}}}{m_{\text{Li}}+m_{\text{He}}} \approx \frac{7}{11}Q = 1.77 \text{ MeV}$$

$$\frac{\vec{p}_1^2}{2m_1} + \frac{\vec{p}_2^2}{2m_2} = \frac{-\vec{p}_1^2}{2m_1}\left(1 + \frac{m_1}{m_2}\right) = Q \qquad T({}^7\text{Li}) = \frac{m_{\text{He}}}{m_{\text{Li}}+m_{\text{He}}} \approx \frac{4}{11}Q = 1.01 \text{ MeV}$$

Gadolinium: $n + {}^{155}\text{Gd} \rightarrow \text{Gd}^* \rightarrow \gamma$-ray cascade (mostly continuum), total energy 8.5 MeV

              $n + {}^{157}\text{Gd} \rightarrow \text{Gd}^* \rightarrow \gamma$-ray cascade (mostly continuum), total energy 7.9 MeV
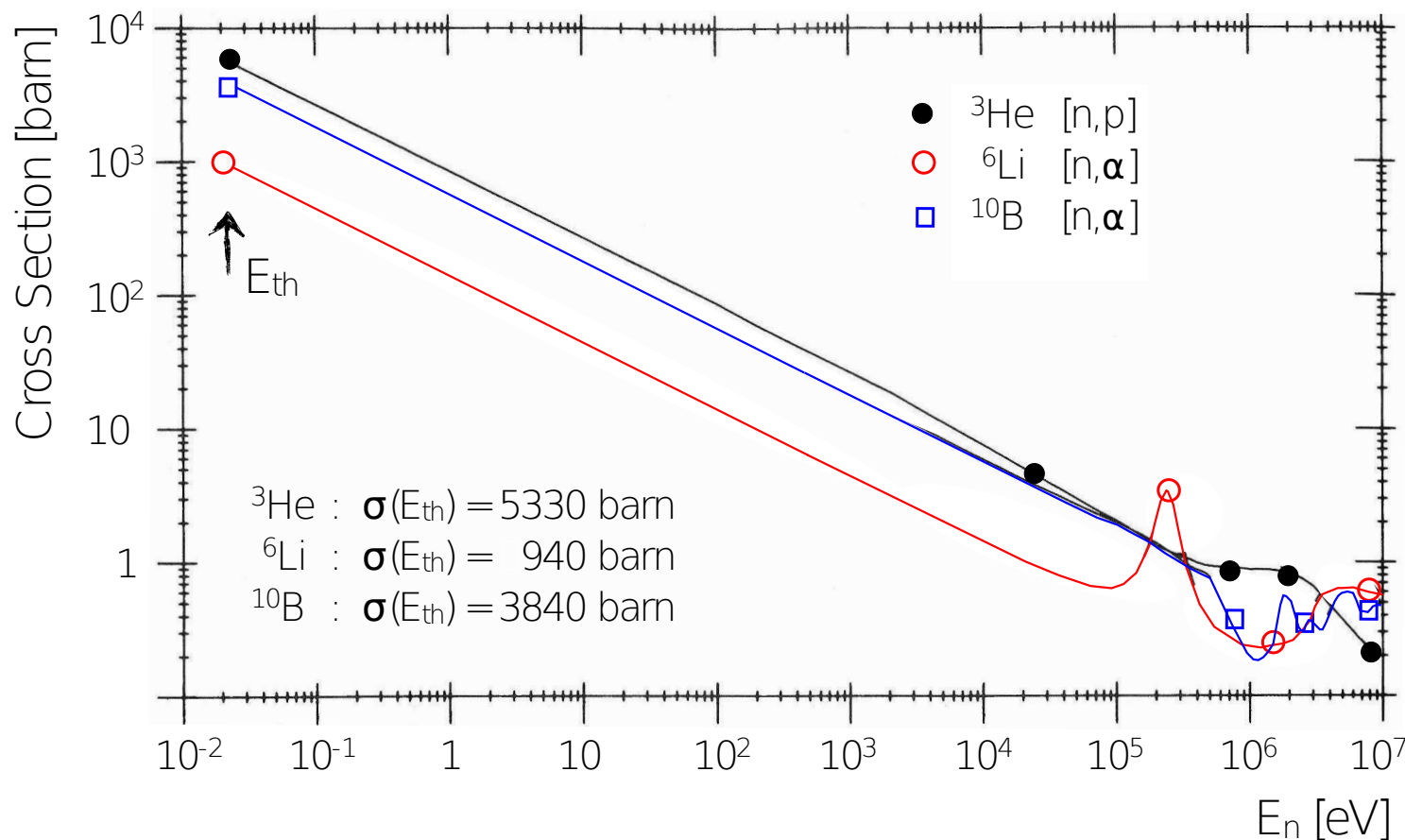
Uranium: $n + {}^{235}\text{U} \rightarrow$ fission fragments (T=170 MeV) + neutrons

Plutonium: $n + {}^{239}\text{Pu} \rightarrow$ fission fragments (T=176 MeV) + neutrons

Detection of Neutrons

cross section for neutron capture process (apart from resonances)

$$\sigma(E) \approx \sigma(E_{\mathrm{th}}) \frac{v_{\mathrm{th}}}{v}$$

interpretation:

cross section increases with time neutron is close to absorbing nucleus

$\rightarrow v^{-1}$-dependence

- ● ^{3}He [n,p]
- ○ ^{6}Li [n,α]
- □ ^{10}B [n,α]

^{3}He : $\sigma(E_{\mathrm{th}}) = 5330$ barn
^{6}Li : $\sigma(E_{\mathrm{th}}) = 940$ barn
^{10}B : $\sigma(E_{\mathrm{th}}) = 3840$ barn

Detection of Neutrons

scintillation detectors: detect scintillation light produced in capture process

e.g. Lithium glass:

$n + {}^6Li \rightarrow {}^4He + {}^3H + 4.79$ MeV

common scintillators used for neutron detection

	density of ^{6}Li atoms [10^{22} cm^{-3}]	scintillation efficiency [in %]	photon wavelength [nm]	photons per neutron
Lithium glass (Ce)	1.75	0.45	395	7000
LiI(Eu)	1.83	2.8	470	51 000
ZnS(Ag)-LiF	1.18	9.2	450	160 000
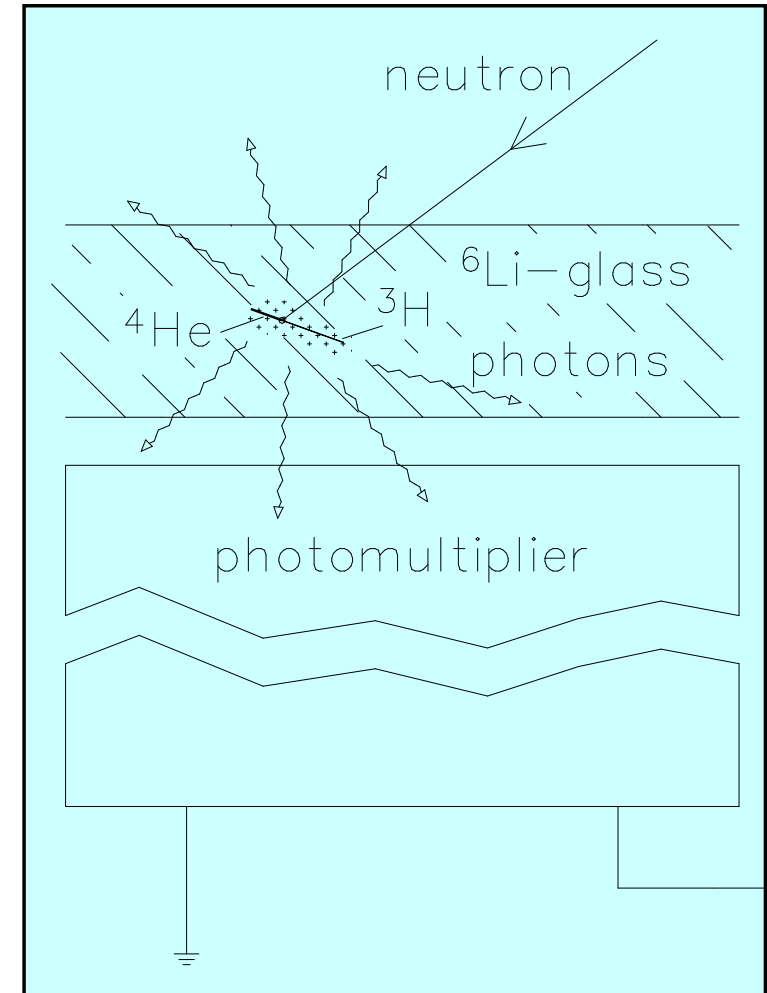
Detection of Neutrons

gas detectors: standard Geiger counter with ^{3}He or BF$_3$ gas

e.g. Helium: $n + {}^3He \rightarrow {}^3H + {}^1H + 0.76$ MeV
 (about 25 000 ionizations produced per neutron, charge ≈ 4 fC)
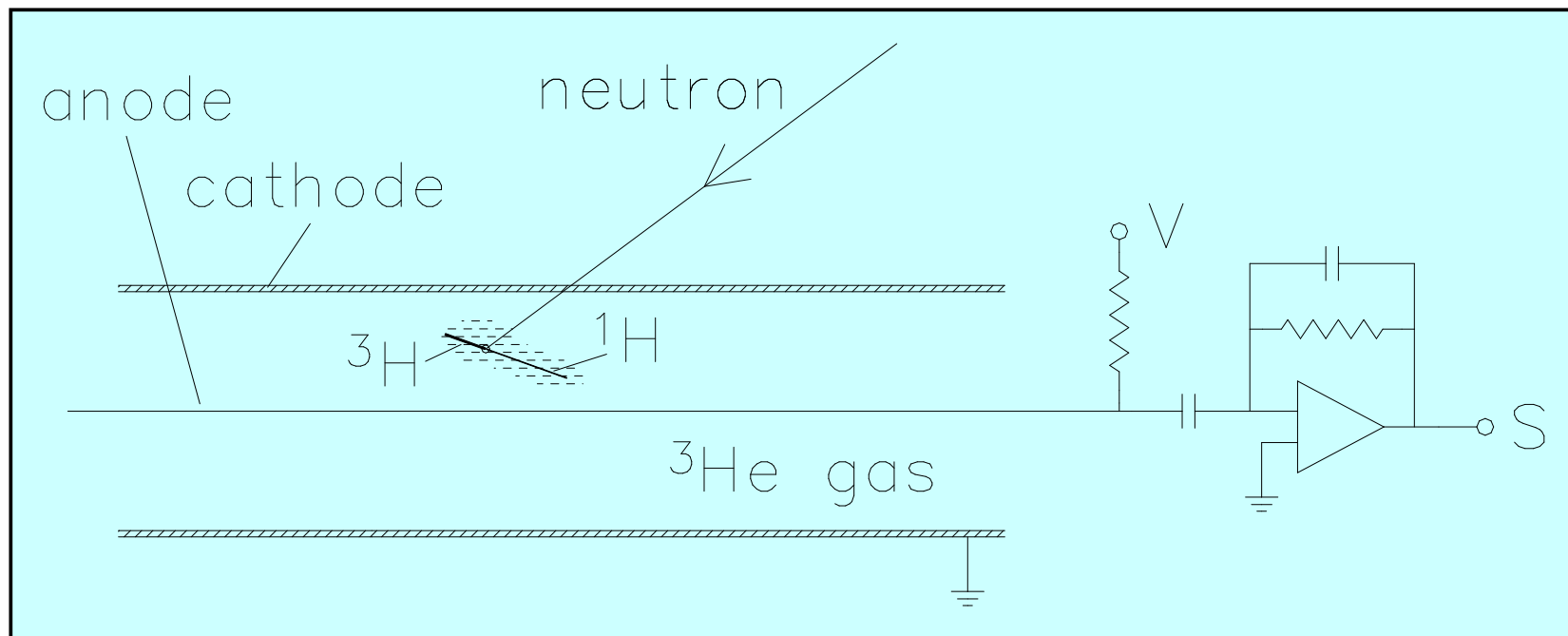
Detection of Neutrons

wall effect:

$$n + {}^3He \rightarrow {}^3H + {}^1H + 0.76 \text{ MeV}$$
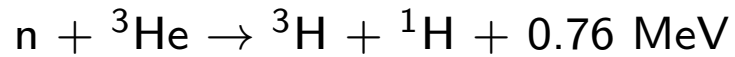
from mass ratio
$T_p = 573$ keV (p = ^{1}H)
$T_t = 191$ keV (t = ^{3}H)

ranges:

Si: $R_p \approx 6\mu$m, $R_t \approx 5\mu$m
gas: few mm ($\sim 1000 \times R_{\mathrm{solid}}$)

remark: energy spectrum reflects detector
response, not neutron energy
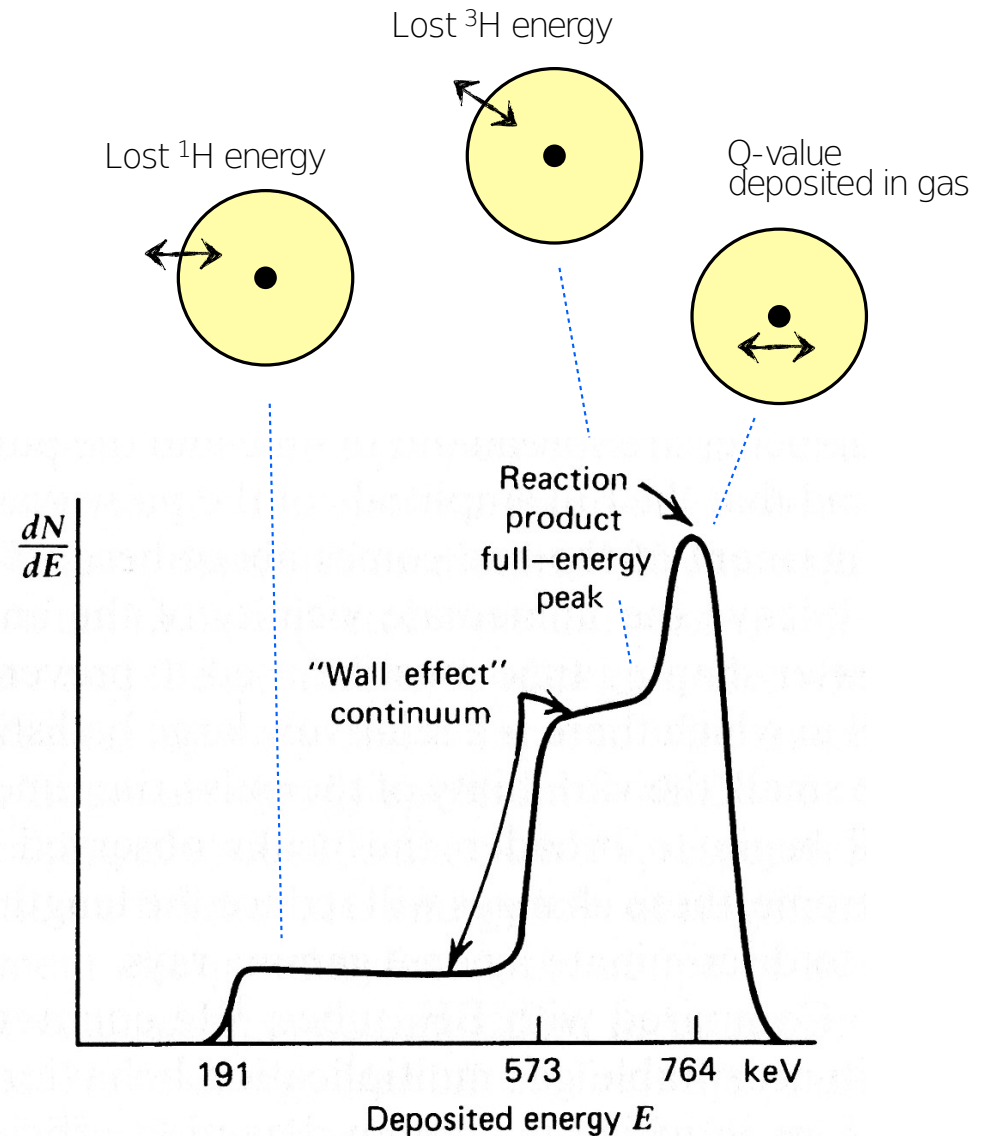
Detection of Neutrons
Fast Neutrons

generally, detection relies on observing neutron-induced nuclear reactions

capture cross sections for fast-neutron induced reactions are small
compared to those at low energies; remember: $\sigma_{\mathrm{cap}} \propto 1/v$

two approaches to detect fast neutrons:

- thermalize/moderate & capture as before, only providing count rates (i.e. neutron flux)

- elastic scattering off protons at high energy
  - protons are easy to detect in conventional detectors
  - observe recoils for time-of-flight (ToF), enables
    neutron energy measurements by measuring the velocity

Detection of Neutrons
Neutron Moderation

- moderate neutrons to increase efficiency in conventional slow-neutron detector
- hydrogen-rich materials: polyethylene or paraffin

optimum thickness between few cm to tens of cm
for energies of keV to MeV

trade-off between sufficient slow down
and detection cross section
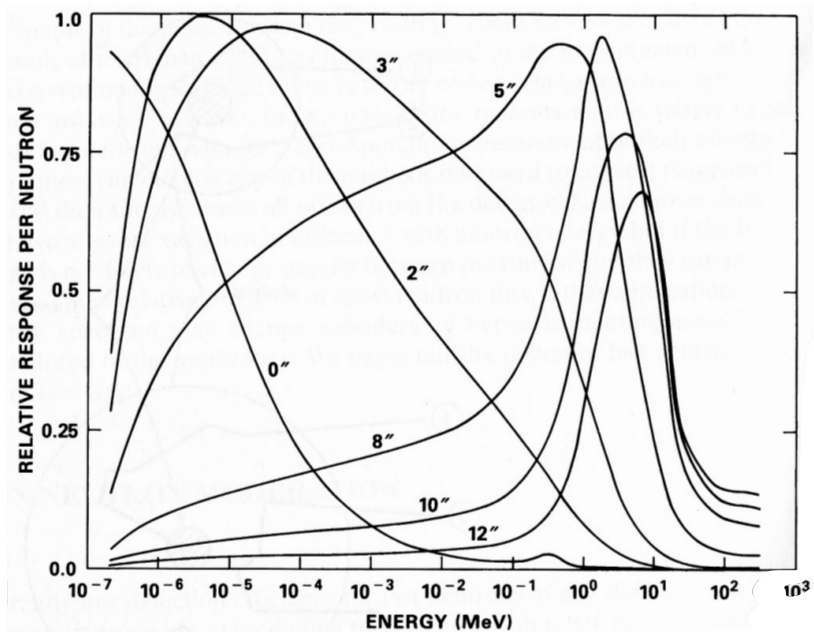
Relative response vs. energy for
various absorber thicknesses (in inch)
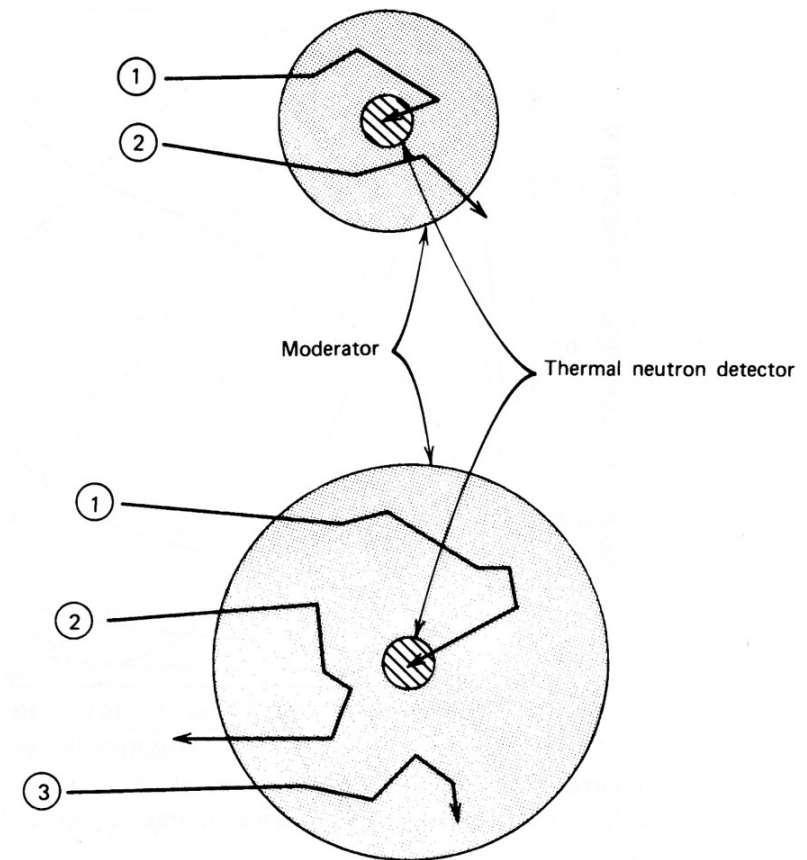
Detection of Neutrons
The Bonner Sphere - Tom W. Bonner et al., 1960

10-12" diameter moderator sphere with LiI(Eu) scintillator in center, has a similar response curve as the neutron rem dose curve in tissue

application:

several spheres of diff. size → neutron spectrum
single sphere of appropriate size: determination of dose equivalent due to neutrons with an unknown or variable neutron spectrum
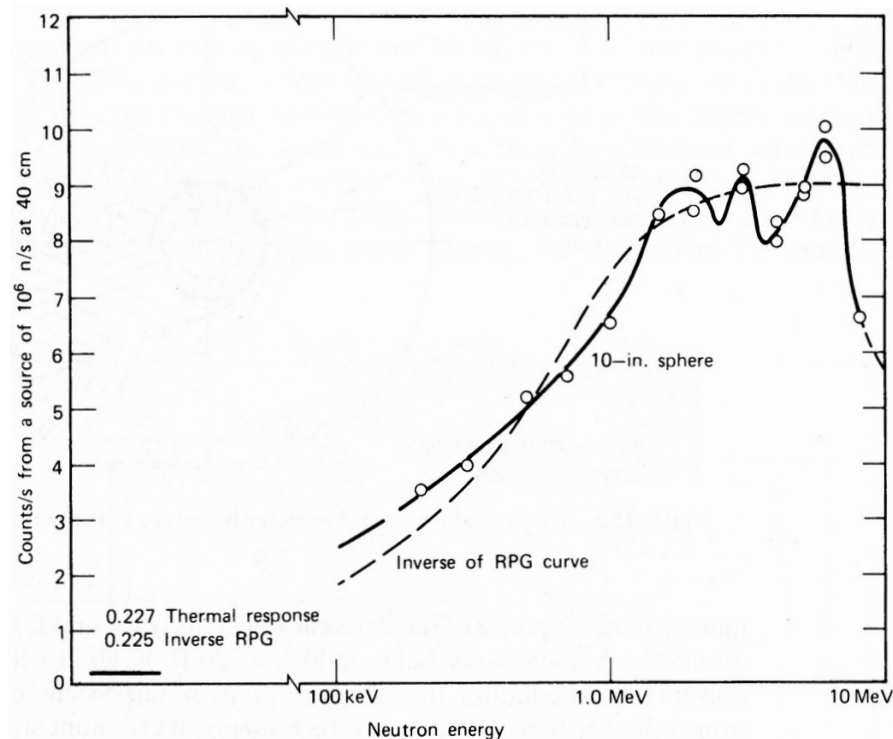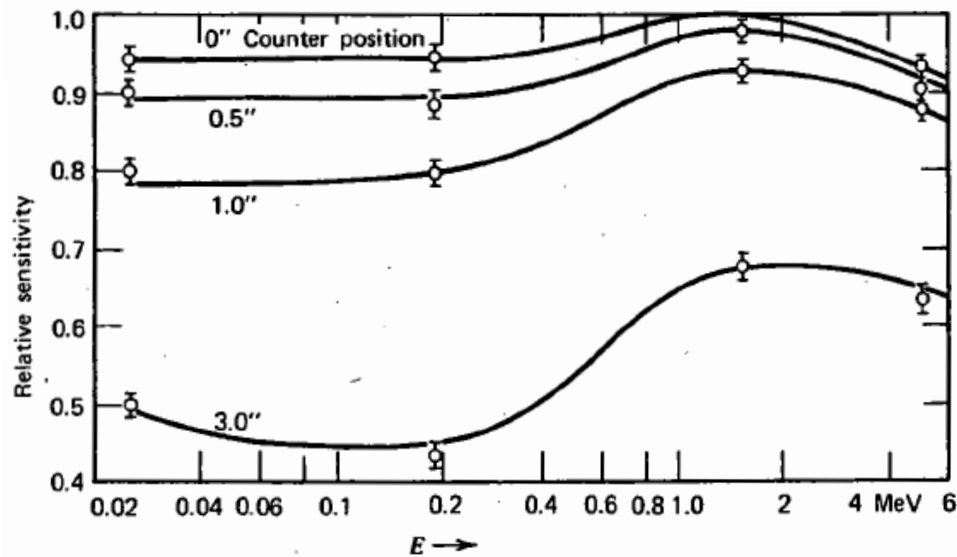
Detection of Neutrons
The Long Counter

neutron energy independent efficiency:
'flat response'

slow-neutron BF_3 detector in center of device
paraffin moderator, B_2O_3 absorber (shielding)

only sensitive to neutrons from one side

relative sensitivity of Long Counter
varied parameter is the distance of the end of
the BF_3 tube if shifted in from the front of the
moderator face
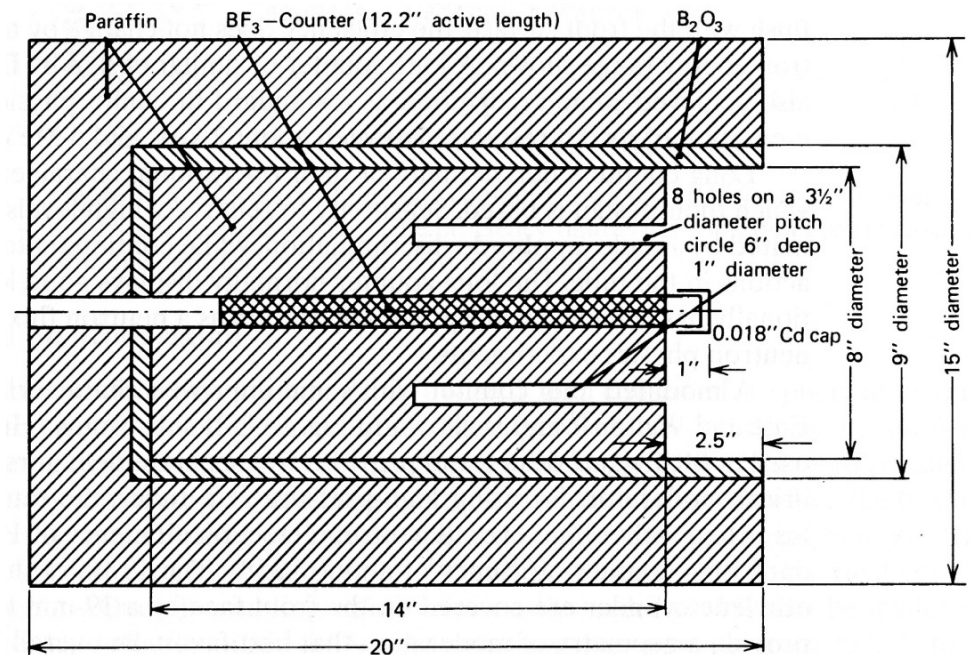
cross section of Long Counter

cencentric holes prevent efficiency reduction for
neutrons with energies below 1 MeV

Detection of Neutrons

| detector type	size	neutron active material	incident neutron energy	neutron detection efficiency[a] (%)	γ-ray sensitivity (R/h)[b]
plastic scintillator	5 cm thick	^{1}H	1 MeV	78	0.01
liquid scintillator	5 cm thick	^{1}H	1 MeV	78	0.1
loaded scintillator	1 mm thick	^{6}Li	thermal	50	1
Hornyak button	1 mm thick	^{1}H	1 MeV	1	1
CH_4 (7 bar)	5 cm Ø	^{1}H	1 MeV	1	1
^{4}He (18 bar)	5 cm Ø	^{4}He	1 MeV	1	1
^{3}He (4 bar), Ar (2 bar)	2.5 cm Ø	^{3}He	thermal	77	1
^{3}He (4 bar), CO_2 (5%)	2.5 cm Ø	^{3}He	thermal	77	10
BF_3 (0.66 bar)	5 cm Ø	^{10}B	thermal	29	10
BF_3 (1.18 bar)	5 cm Ø	^{10}B	thermal	46	10
^{10}B-lined chamber	0.2 mg/cm^3	^{10}B	thermal	10	10^3
fission chamber	1.0 mg/cm^3	^{235}U	thermal	0.5	$10^6 - 10^7$

[a] interaction probability for neutrons of the specified energy, normal incidence angle
[b] approximate upper limit of γ-ray dose that can be present with the detector still providing usable neutron output signals

Detection of Neutrons

Cascade Detector

capture process:

$$n + {}^{10}B \rightarrow {}^{7}Li^* + {}^{4}He + 2.31 \text{ MeV } (93\%)$$
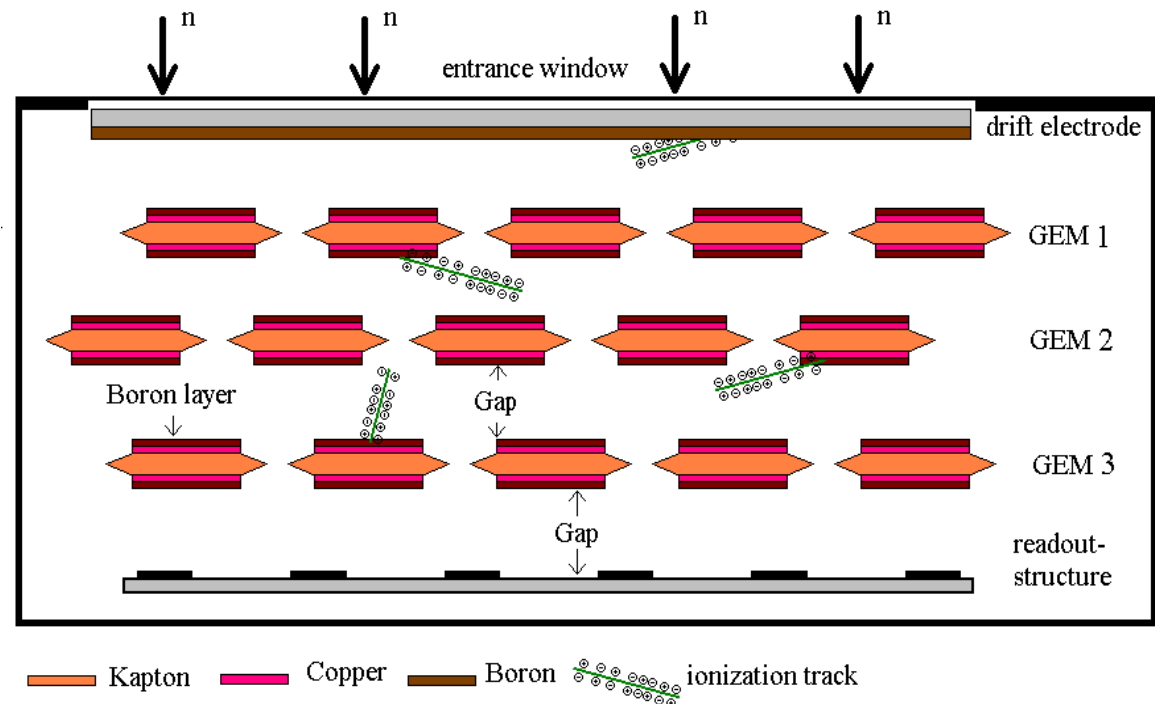$$\rightarrow {}^{7}Li + {}^{4}He + 2.78 \text{ MeV } (7\%)$$
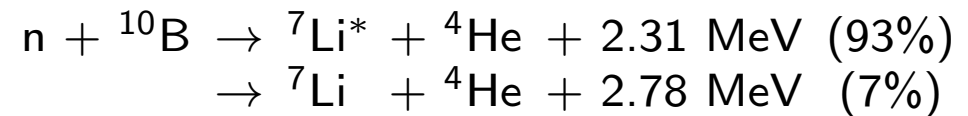
Setup:

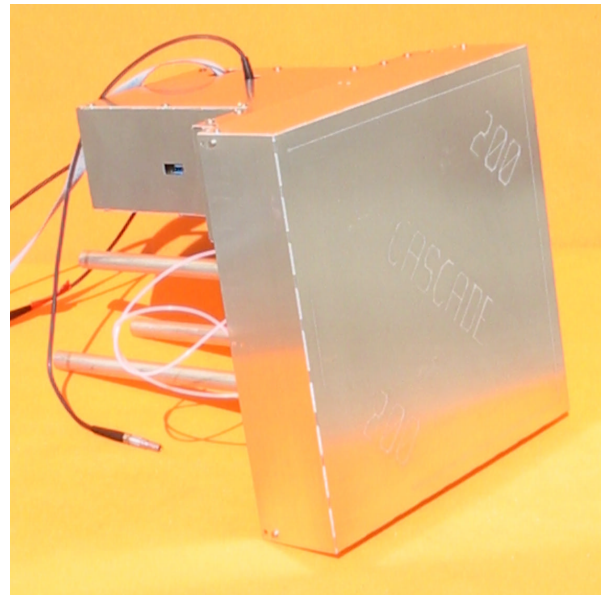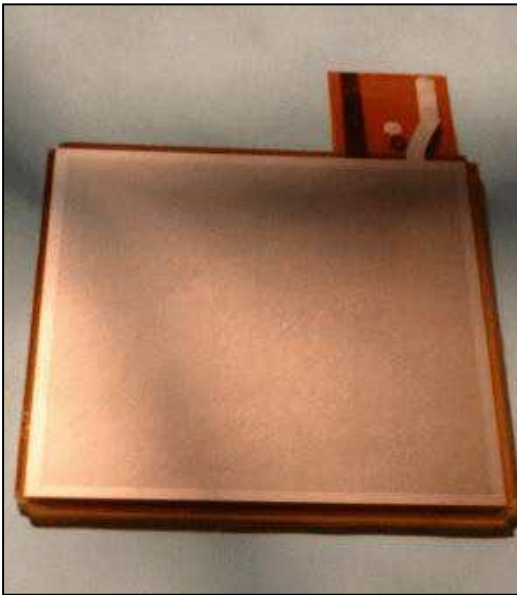Boron layers on multiple GEM foils

GEMs:

- operated to be transparent for produced charges
- can be cascaded
- two Boron layers each
- last one: amplification layer
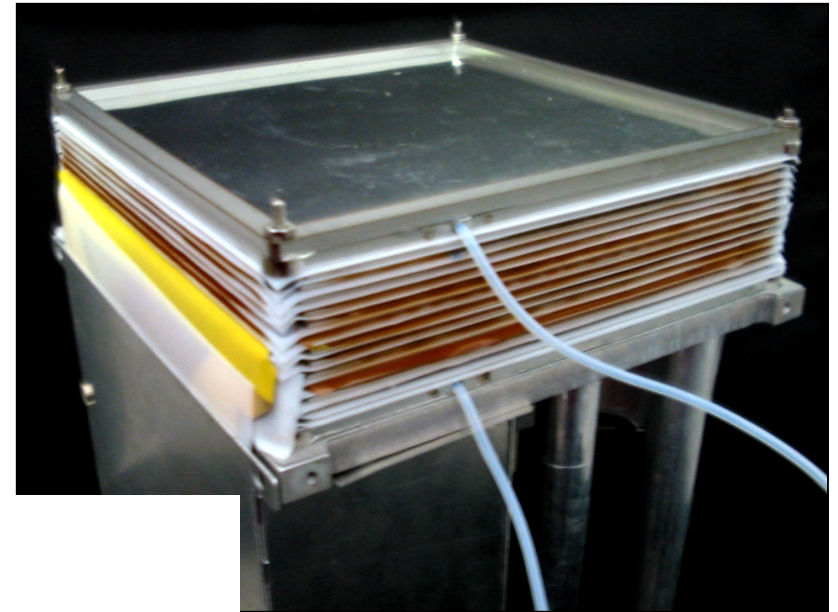- high rate capability [10^7 Hz/cm^2]

CASCADE neutron detector schematic

Detection of Neutrons
CASCADE Detector, M. Klein, C. Schmidt NIM A628 (2011) 9

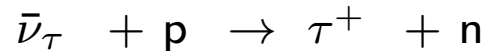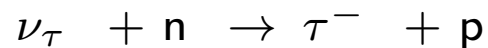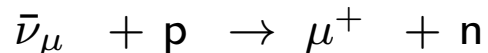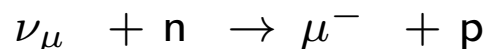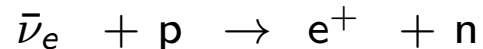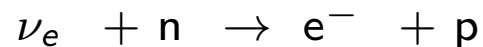GEM foil glued to frame, complete CASCADE module

Cascade neutron detector: several GEM-modules stacked with drift electrodes and readout

10.3 Detection of Neutrinos

neutrino detection only via weak interaction
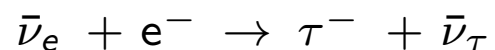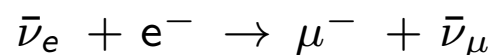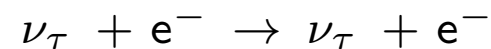
Charged Current

Neutral Current

possible reactions:

charged current reactions:

$$\nu_e + n \rightarrow e^- + p$$
$$\bar{\nu}_e + p \rightarrow e^+ + n$$
$$\nu_\mu + n \rightarrow \mu^- + p$$
$$\bar{\nu}_\mu + p \rightarrow \mu^+ + n$$
$$\nu_\tau + n \rightarrow \tau^- + p$$
$$\bar{\nu}_\tau + p \rightarrow \tau^+ + n$$

. . .

$$\bar{\nu}_e + e^- \rightarrow \mu^- + \bar{\nu}_\mu$$
$$\bar{\nu}_e + e^- \rightarrow \tau^- + \bar{\nu}_\tau$$

neutral current reactions:

$$\nu_e + e^- \rightarrow \nu_e + e^-$$
$$\nu_\mu + e^- \rightarrow \nu_\mu + e^-$$
$$\nu_\tau + e^- \rightarrow \nu_\tau + e^-$$
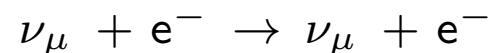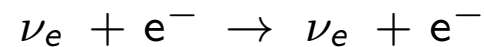
neutrino-nucleon cross section, examples:
10 GeV neutrinos: $\sigma = 7 \cdot 10^{-38}$ cm^2/nucleon
on 10 m Fe-target,
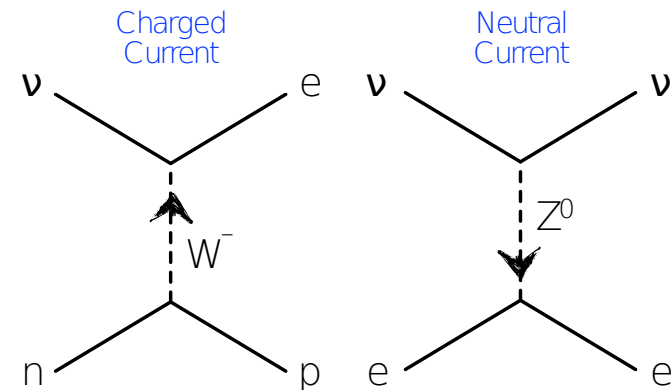interaction probability $P = \sigma N_A d\rho = 3.2 \cdot 10^{-10}$
with $d = 10$ m, $\rho = 7.6$ g/cm^3

solar neutrinos (100 keV): $\sigma = 7 \cdot 10^{-45}$ cm^2/nucleon
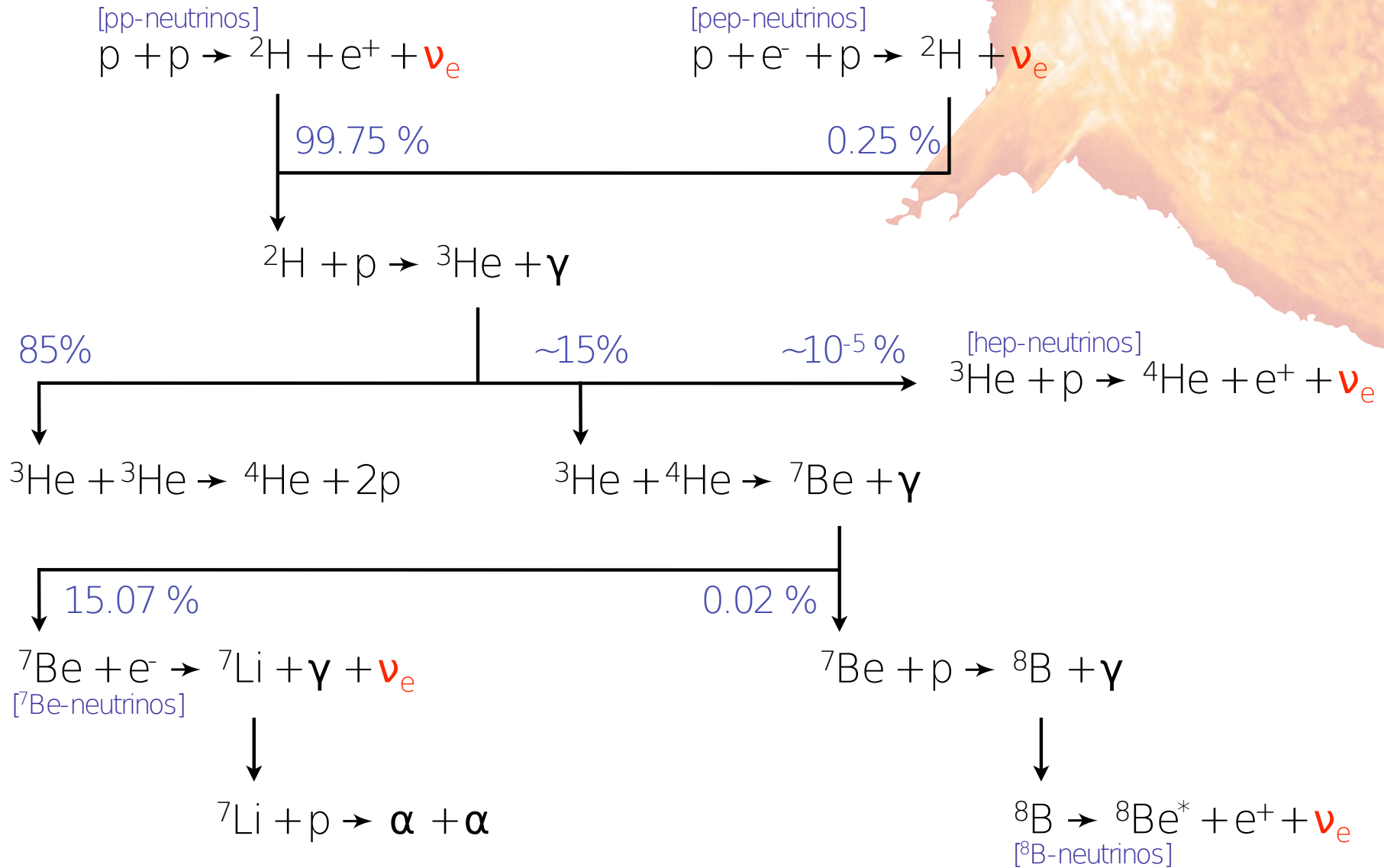through earth, interaction probability: $P = 2.8 \cdot 10^{-11}$
with $d = 12000$ km $= 1.2 \cdot 10^9$ cm, $\rho = 5.5$ g/cm^3

Neutrinos from the Sun (pp chain)

[also: CNO cycle]
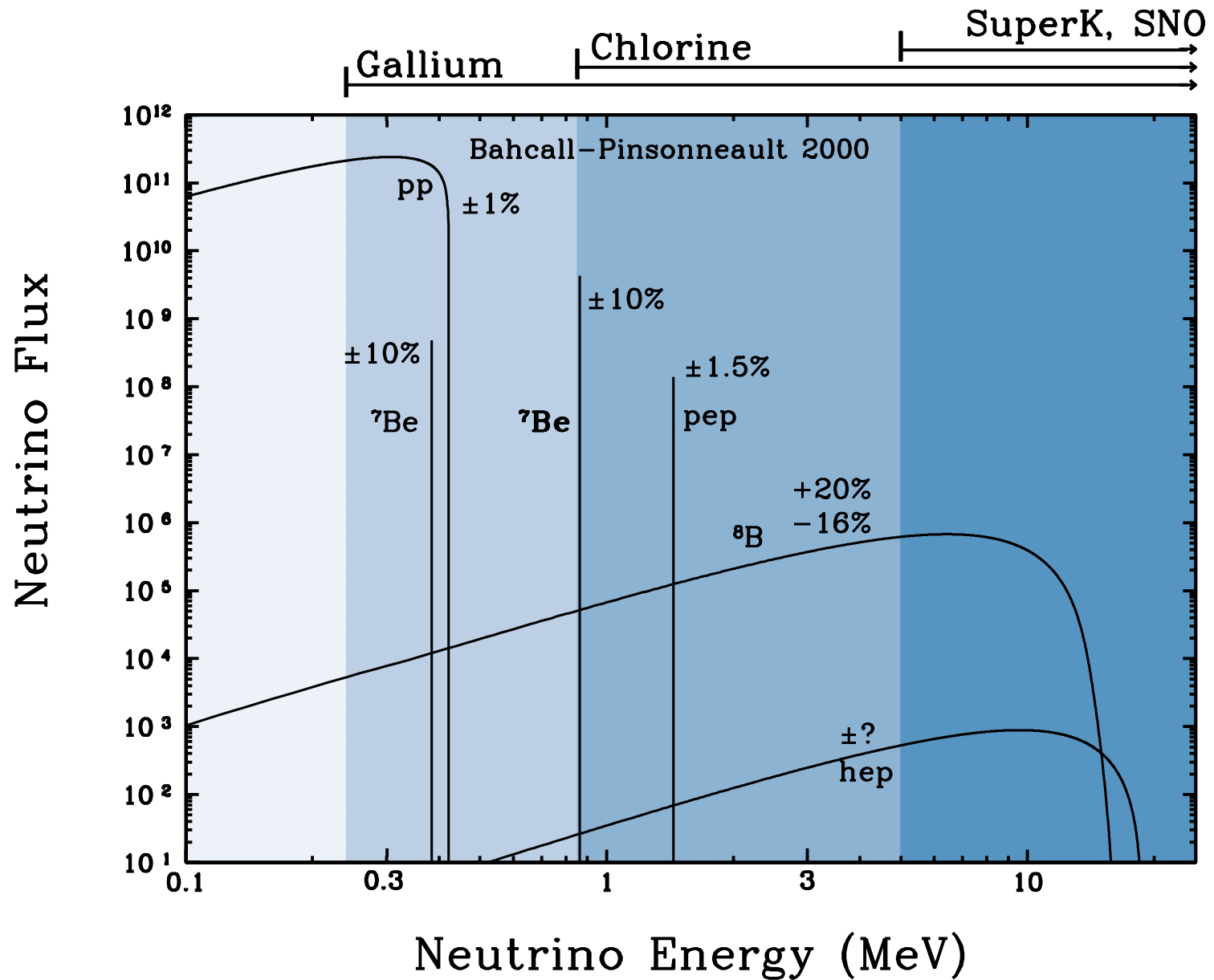
[pp-neutrinos]
$$p + p \to {}^2H + e^+ + \nu_e$$

[pep-neutrinos]
$$p + e^- + p \to {}^2H + \nu_e$$

99.75 %   0.25 %

$$^2H + p \to {}^3He + \gamma$$

85%   ~15%   ~10^{-5} %

[hep-neutrinos]
$$^3He + p \to {}^4He + e^+ + \nu_e$$

$$^3He + {}^3He \to {}^4He + 2p$$ $$^3He + {}^4He \to {}^7Be + \gamma$$

15.07 %   0.02 %

$$^7Be + e^- \to {}^7Li + \gamma + \nu_e$$ $$^7Be + p \to {}^8B + \gamma$$

[^{7}Be-neutrinos]

$$^7Li + p \to \alpha + \alpha$$

$$^8B \to {}^8Be^* + e^+ + \nu_e$$

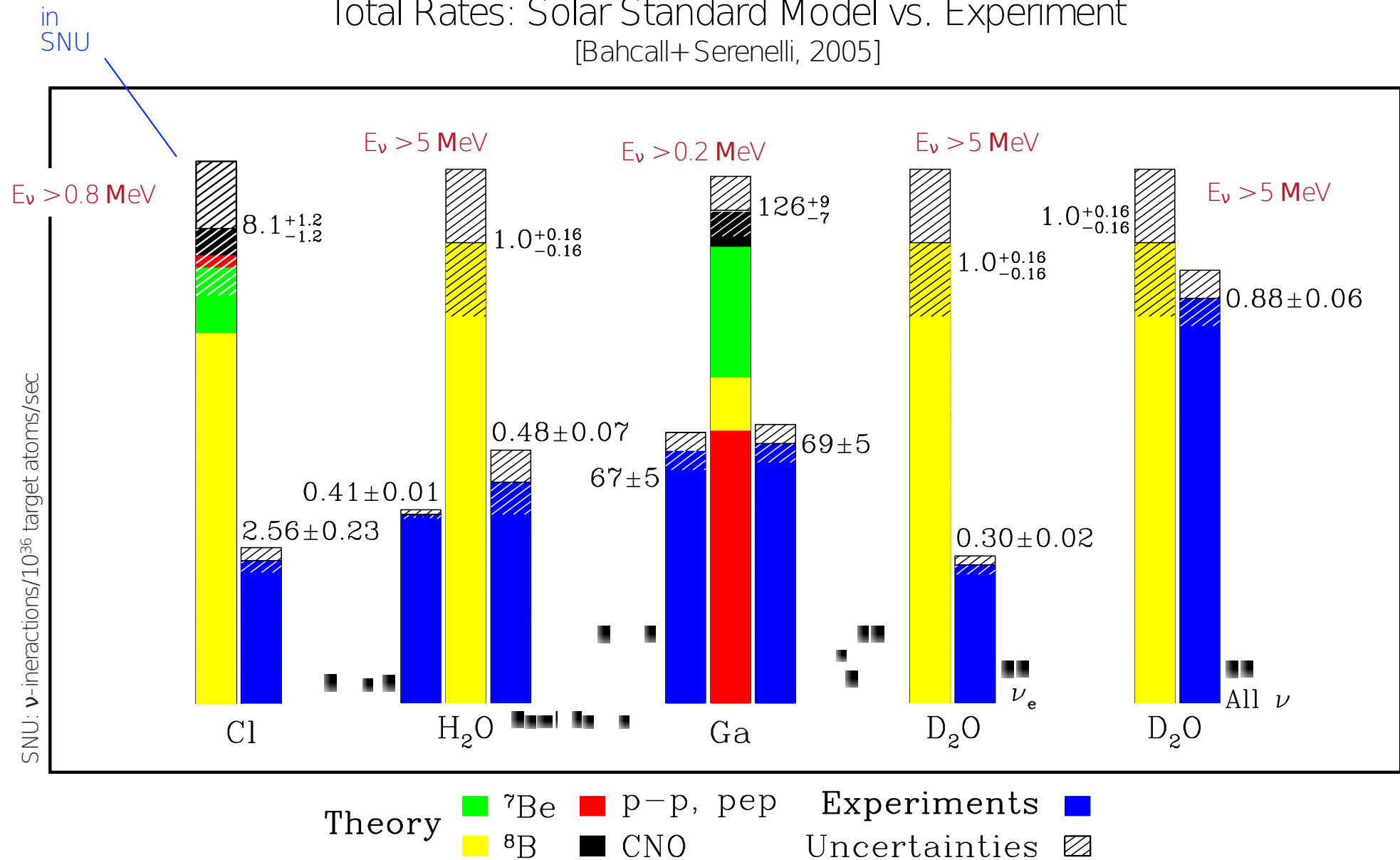[^{8}B-neutrinos]

Neutrinos from the Sun

Solar Electron-Neutrino Problem

in
SNU

Total Rates: Solar Standard Model vs. Experiment
[Bahcall+Serenelli, 2005]

SNU: ν-ineractions/10^{36} target atoms/sec

$E_\nu > 0.8$ MeV

$E_\nu > 5$ MeV

$E_\nu > 0.2$ MeV

$E_\nu > 5$ MeV

$E_\nu > 5$ MeV

$8.1^{+1.2}_{-1.2}$

$1.0^{+0.16}_{-0.16}$

126^{+9}_{-7}

$1.0^{+0.16}_{-0.16}$

$1.0^{+0.16}_{-0.16}$

0.88 ± 0.06

0.48 ± 0.07

0.41 ± 0.01

67 ± 5

69 ± 5

2.56 ± 0.23

0.30 ± 0.02

ν_e

All ν

Cl

H_2O

Ga

D_2O

D_2O

Theory
^{7}Be   p−p, pep   Experiments
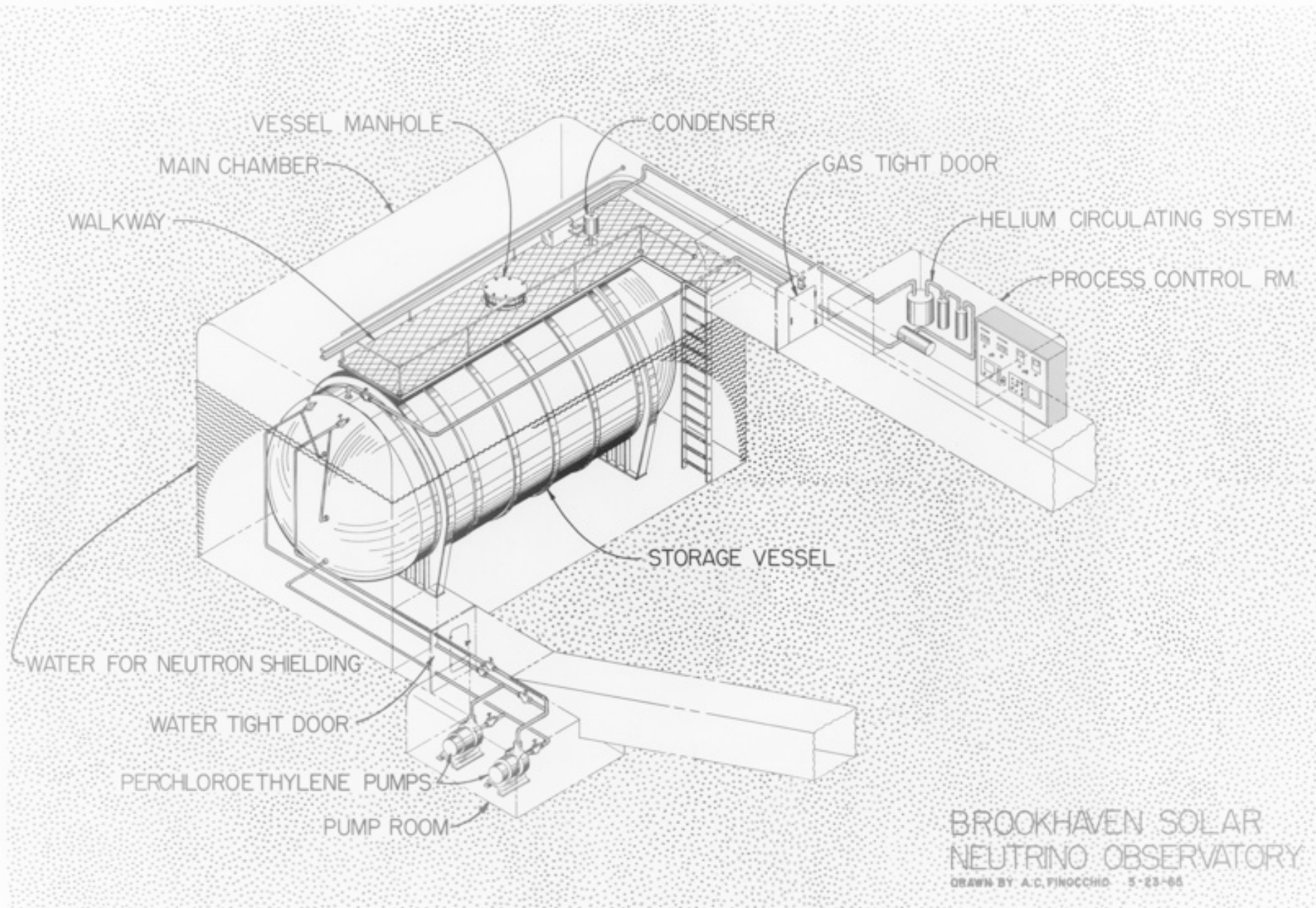^{8}B   CNO   Uncertainties

The Homestake Experiment

the Homestake Gold Mine in South Dakota

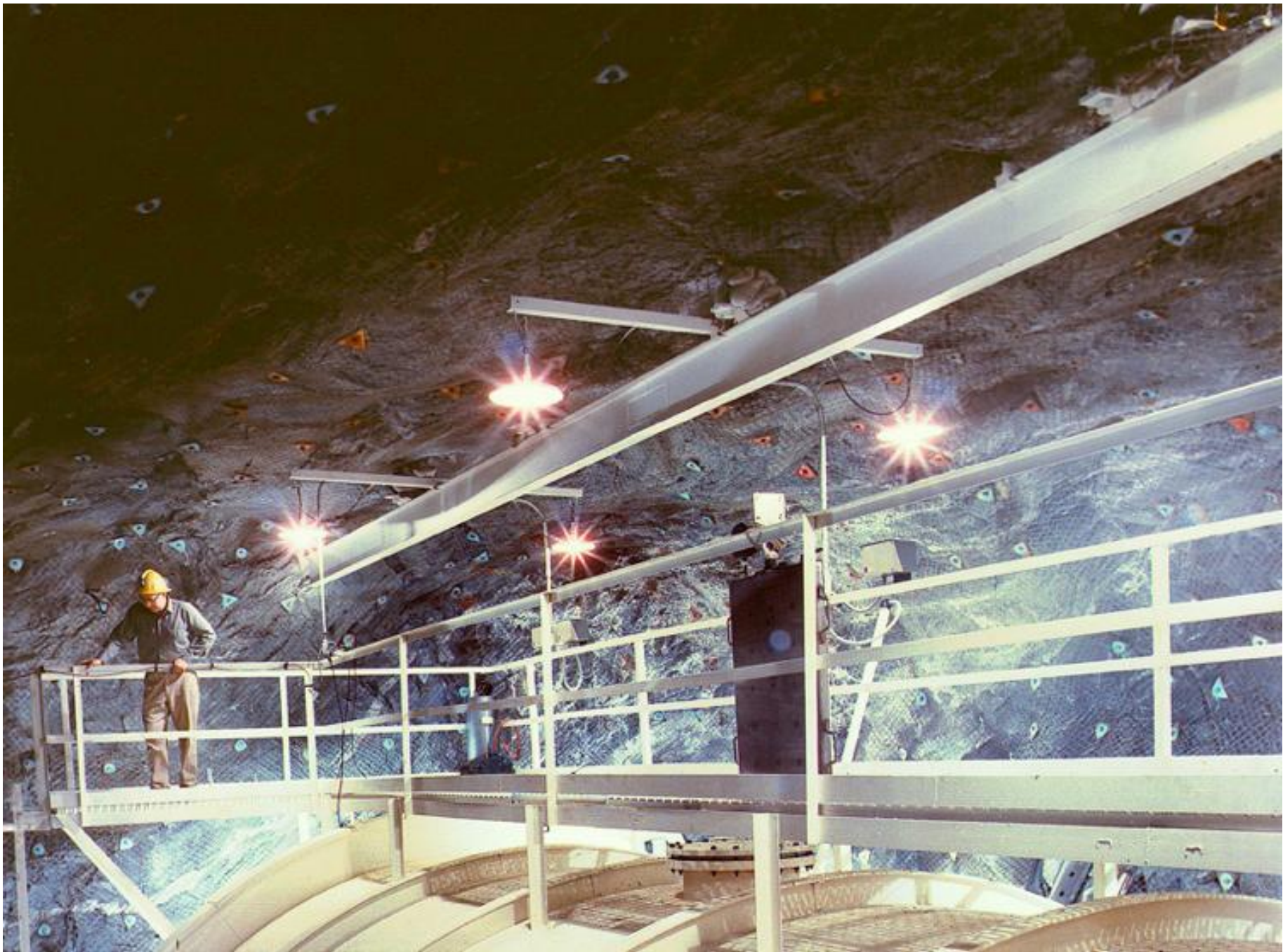
~2500 m
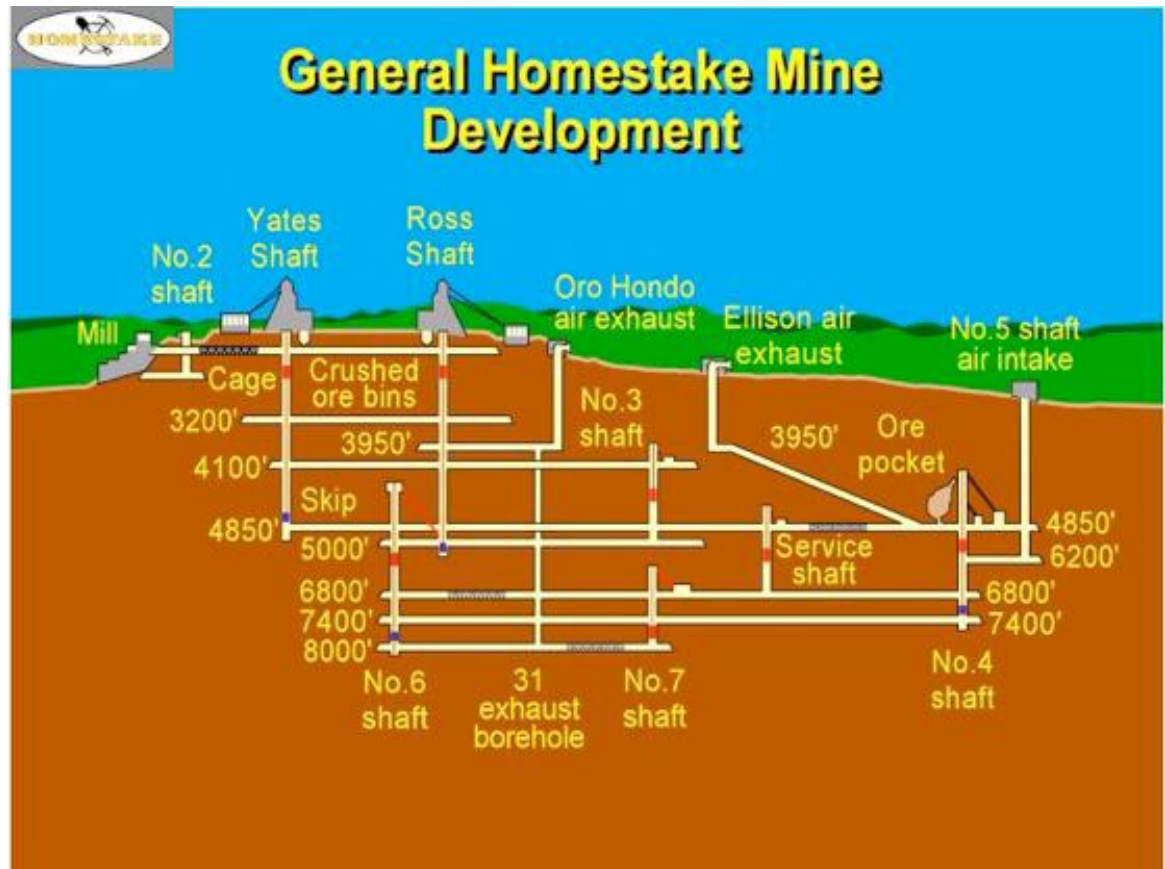
The Homestake Experiment

The Homestake Experiment

Raymond Davis Jr.   construction of the Homestake Mine tank
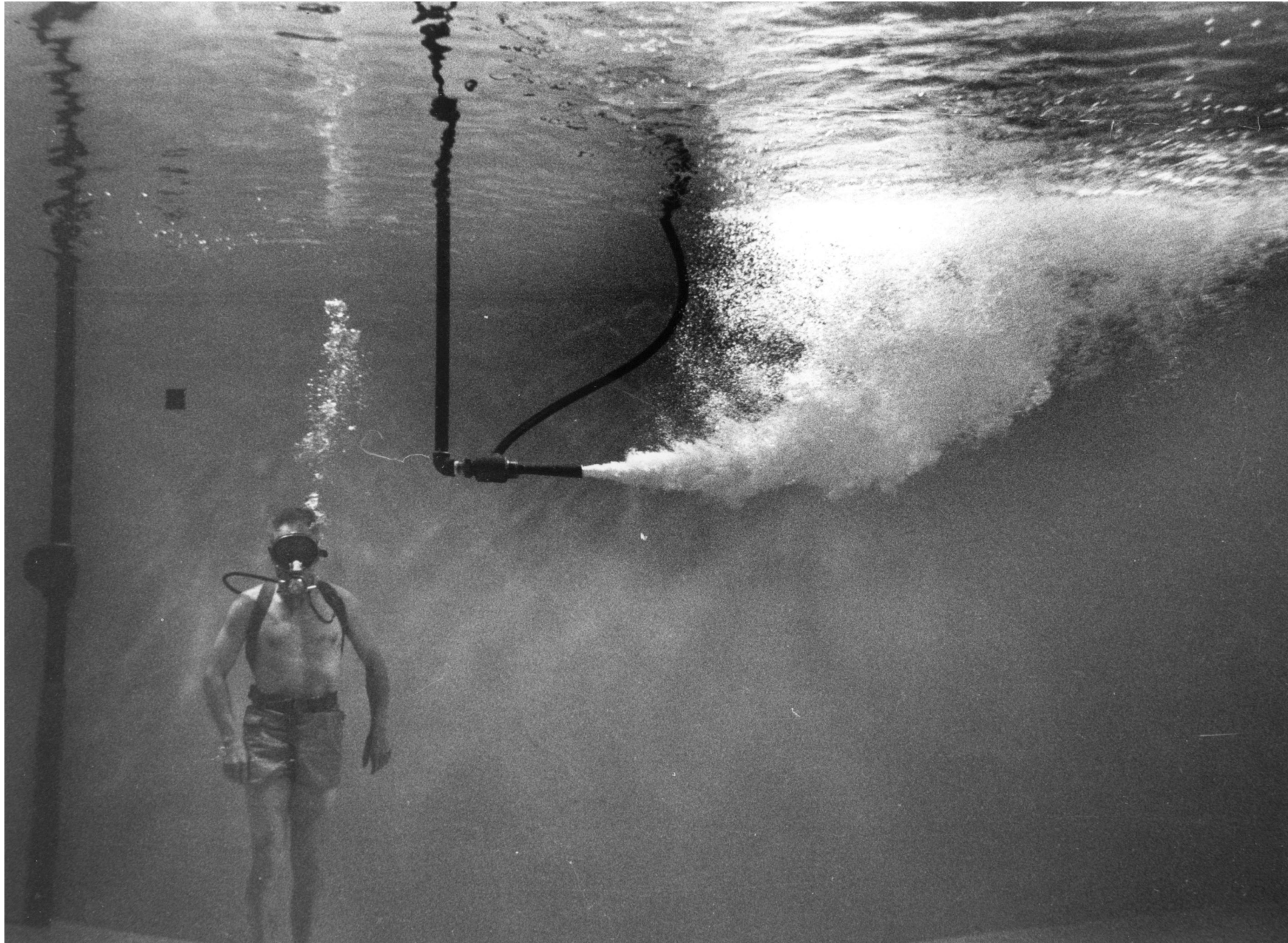
The Homestake Experiment

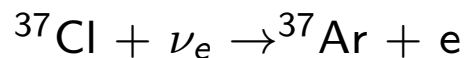# The Homestake Experiment

Raymond Davis Jr.   the eductors being tested in swimming pool at BNL
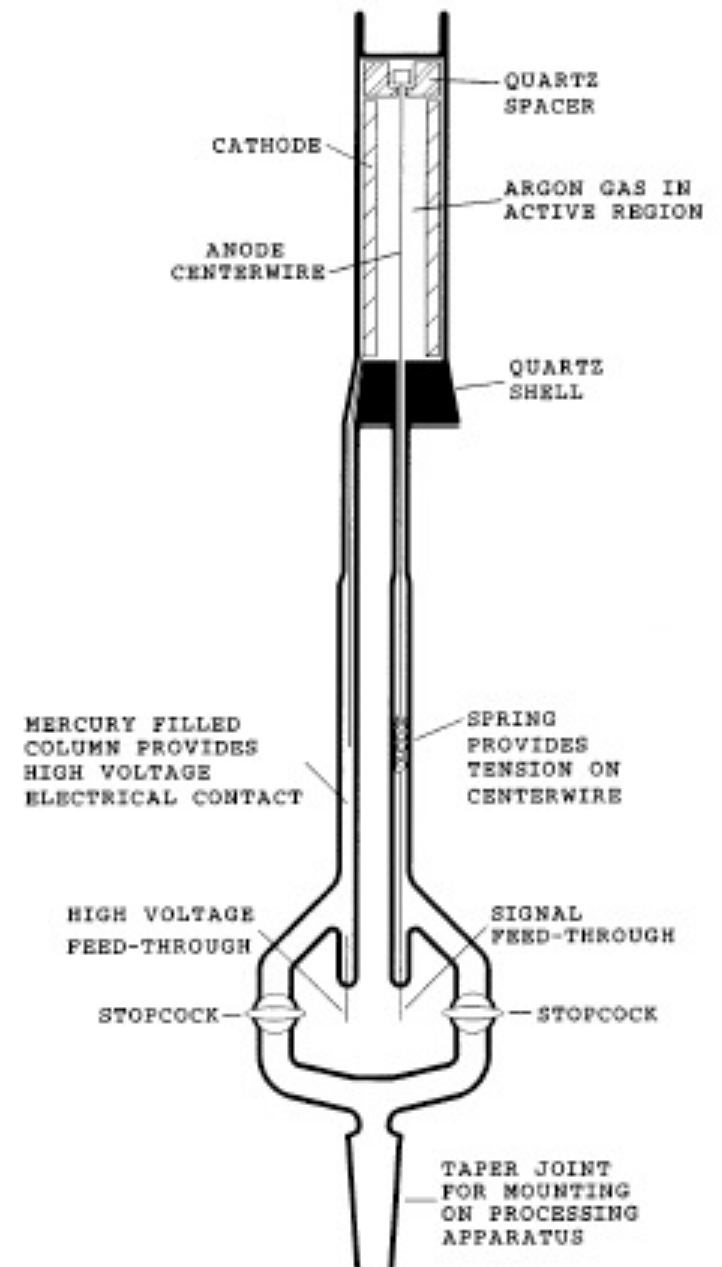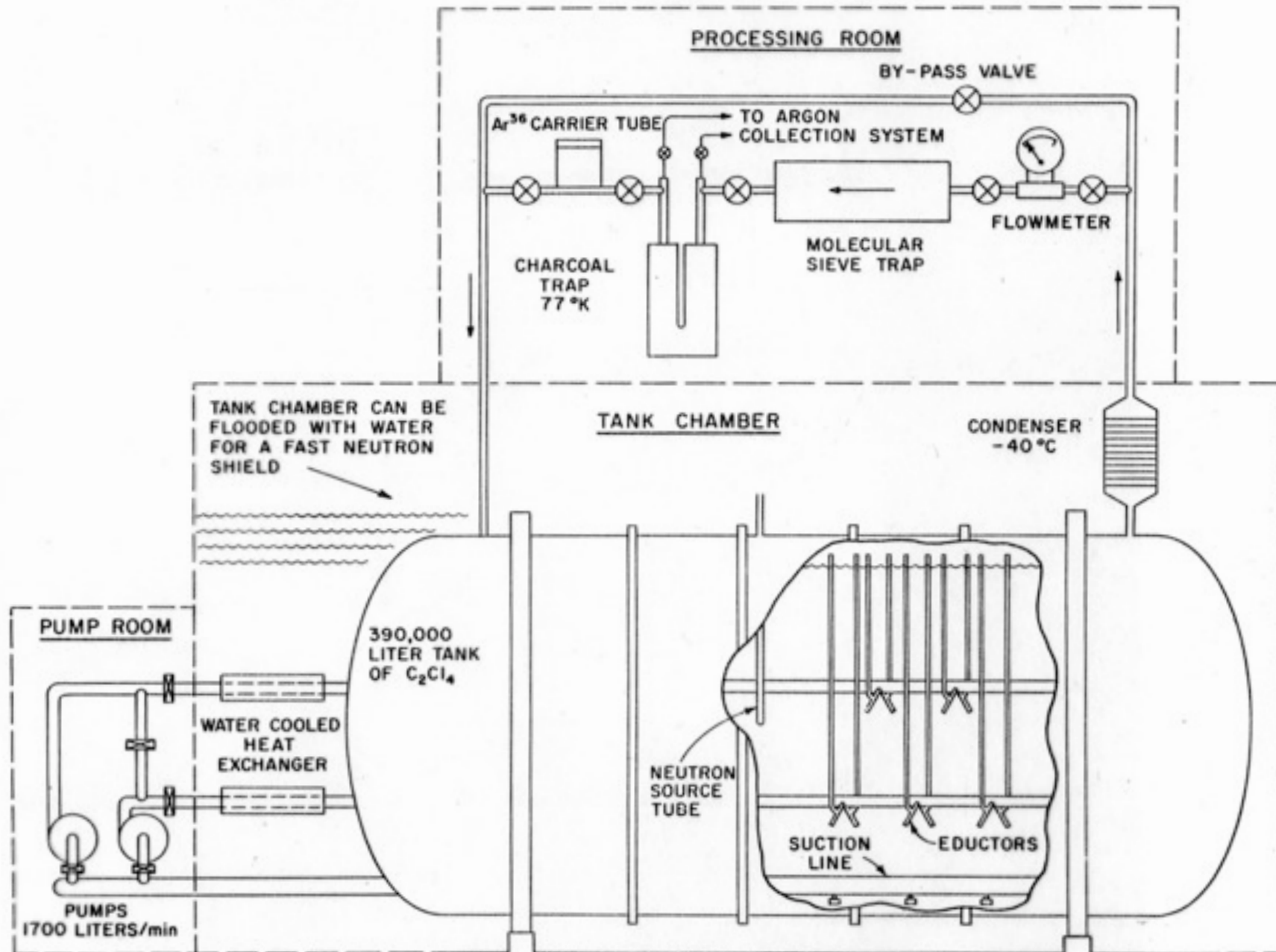
The Homestake Experiment

neutrino capture:

$$^{37}\text{Cl} + \nu_e \to \,^{37}\text{Ar} + e$$

detection of ^{37}Ar via K-shell e^--capture

$$[^{37}\text{Ar}(e,\nu_e)^{37}\text{Cl}] \quad \tau \approx 35 \text{ d}$$

resulting in a 2.82 keV Auger electron
detection after extraction in proportional counter

QUARTZ SPACER

CATHODE

ARGON GAS IN ACTIVE REGION

ANODE CENTERWIRE

QUARTZ SHELL

MERCURY FILLED COLUMN PROVIDES HIGH VOLTAGE ELECTRICAL CONTACT

SPRING PROVIDES TENSION ON CENTERWIRE

HIGH VOLTAGE FEED-THROUGH

SIGNAL FEED-THROUGH

STOPCOCK

STOPCOCK

TAPER JOINT FOR MOUNTING ON PROCESSING APPARATUS

The Homestake Experiment

The Homestake Experiment

some approximate numbers

- 615 tons C_2Cl_4 (tetrachloro-ethylene)

- about $2 \cdot 10^{30}$ chlorine atoms (^{37}Cl)

- prediction: $7.5 \cdot 10^{-36}$ neutrino reactions/atom/s $= 7.5$ SNU

- considering half-life $= 35$ days, expect: 60 atoms every 2 months

- After 25 years: expectation: ≈ 5000 ^{37}Ar atoms expected
  observation: ≈ 2200 ^{37}Ar atoms produced

  [875 counted, 776 after background subtraction]

  ^{37}Ar extraction efficiency: $\approx 95\%$
  ^{37}Ar decay detection efficiency: $\approx 45\%$

The Homestake Experiment
Pulse height Spectra from first runs [1968]
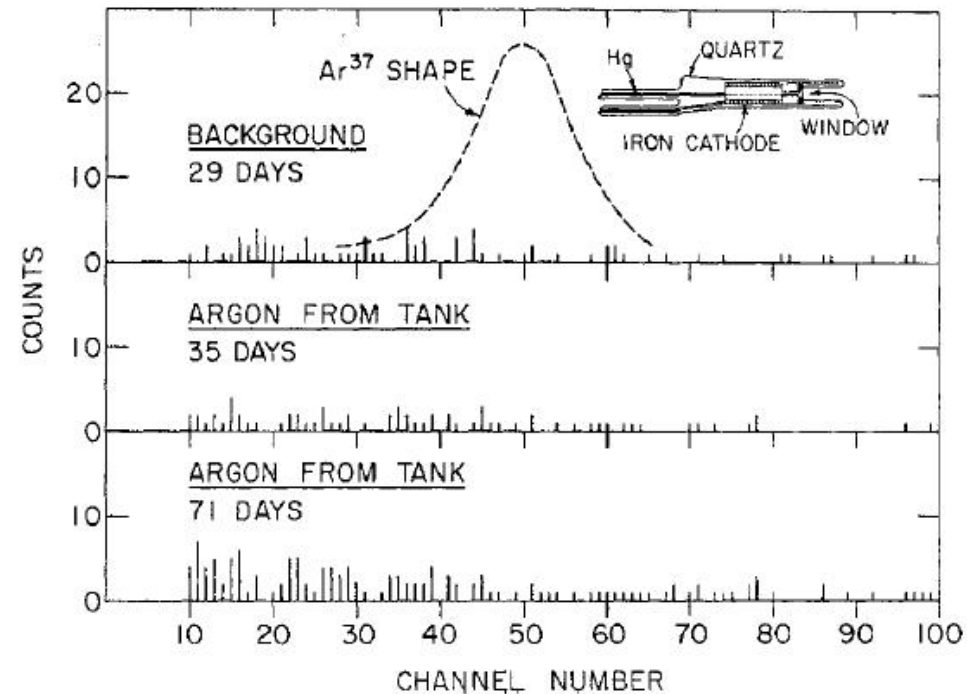
first runs 1968 produced only upper limit of 3 SNU with expectation of 7.5 $\pm$ 3 SNU

solution: pulse shape discrimination

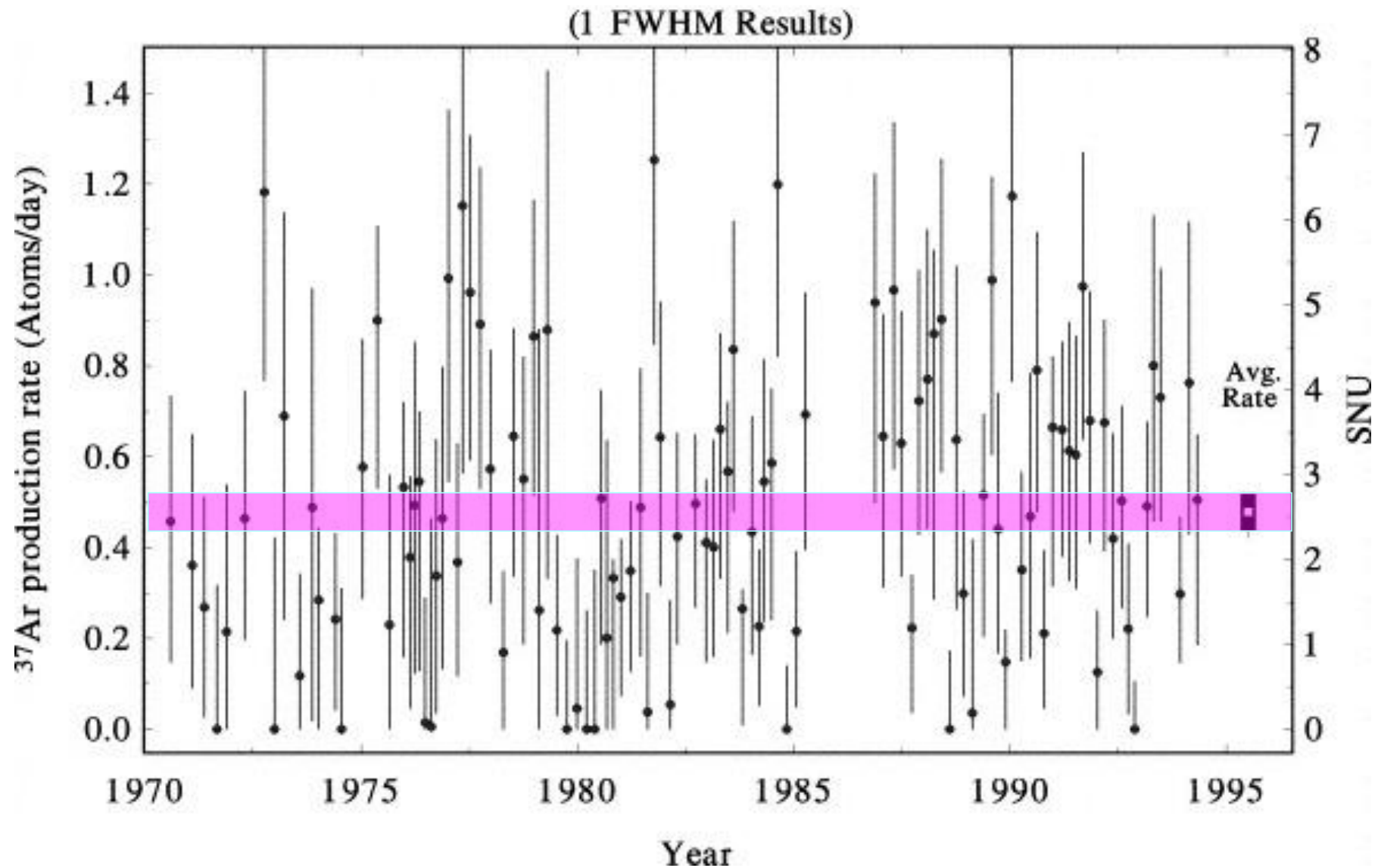signal: 2.82 keV e$^-$ creating about 100 e-ion pairs in 100 μm

background: γ making Compton effect

1970 first observation of solar neutrinos

The Homestake Experiment
Result of 25 years of running

(after implementation of rise time counting)

Nobel Prize 2002

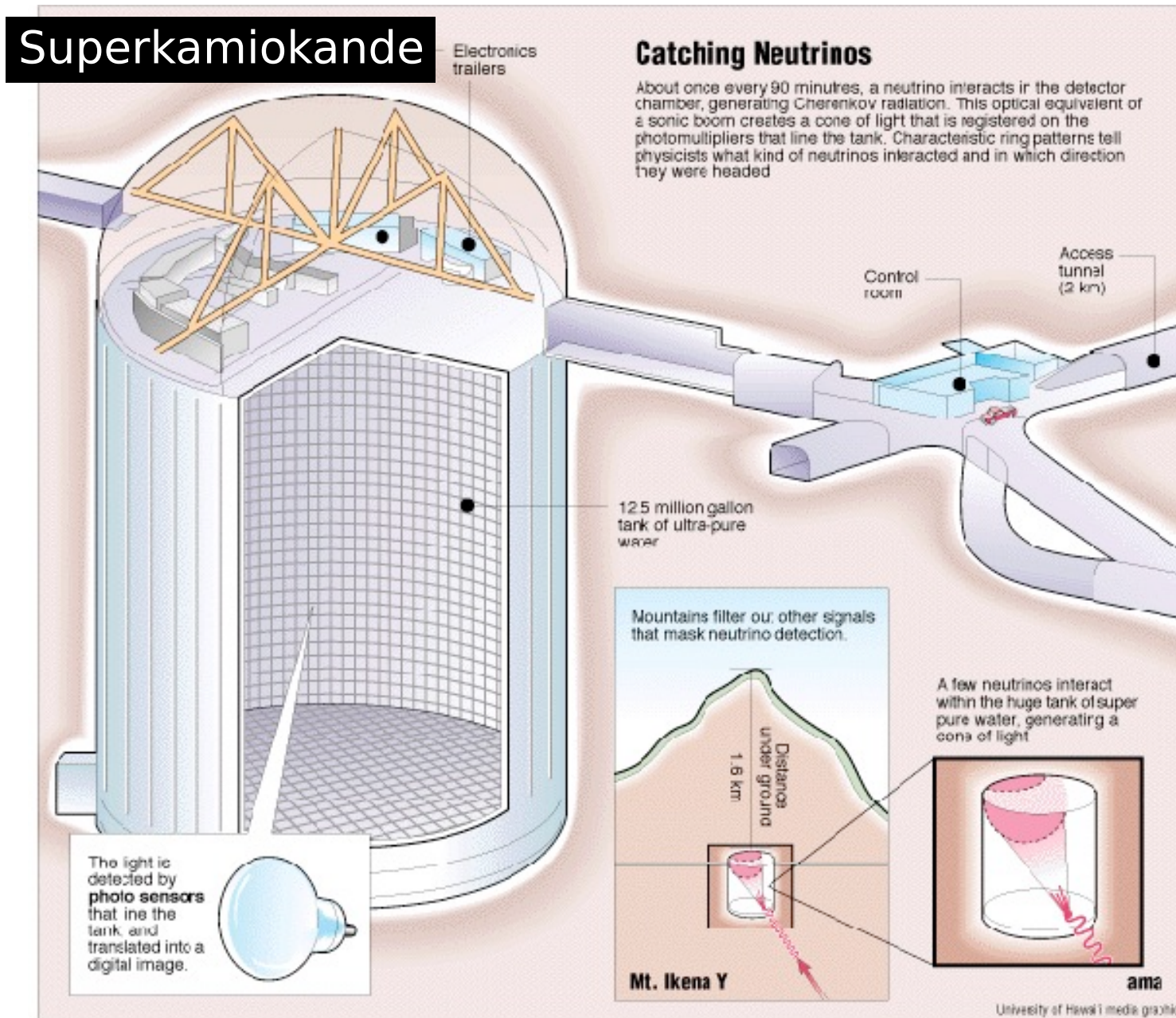Raymond Davis J r. [Homestake]

Masatoshi Koshiba [Kamiokande]

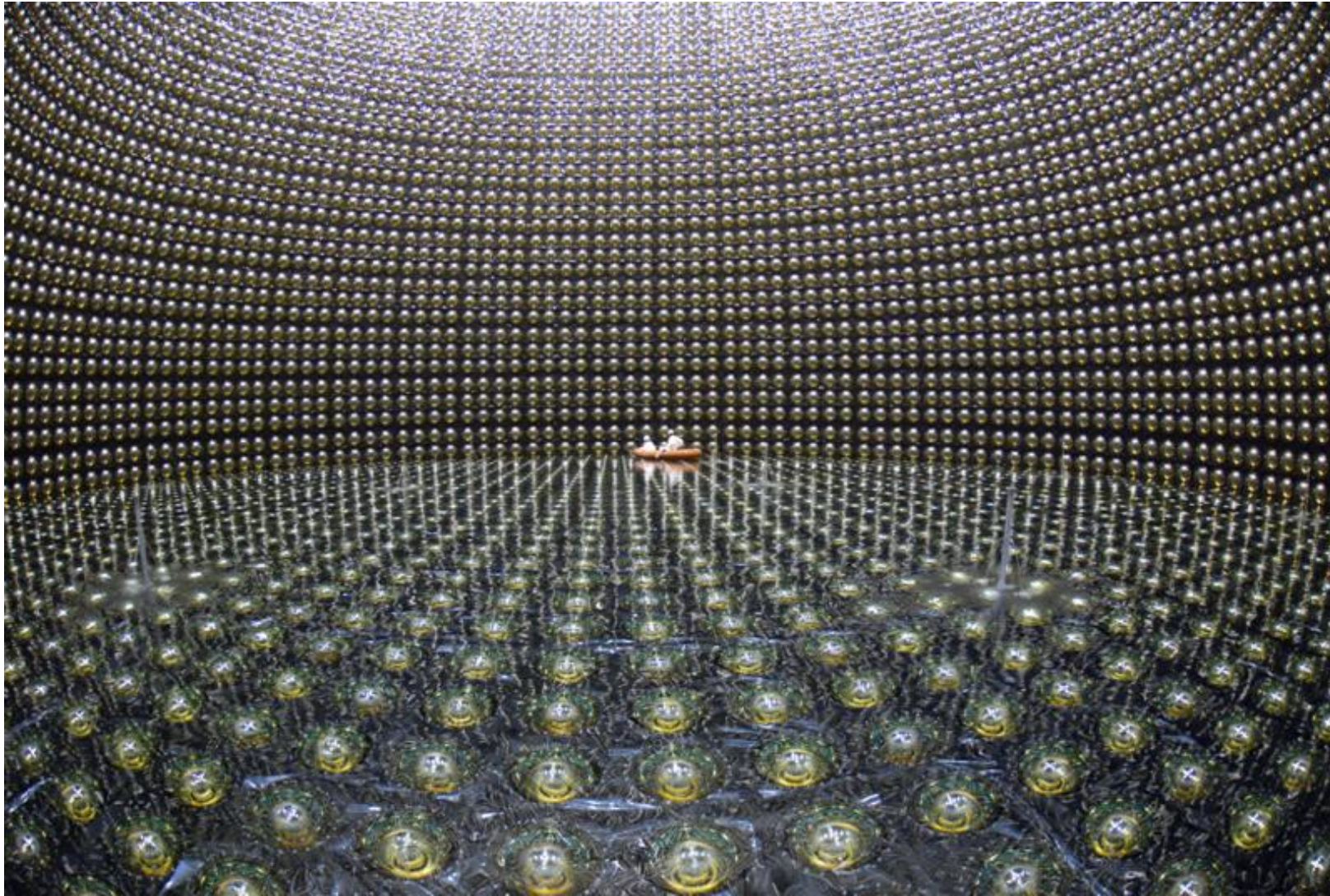Riccardo Giacconi [X-Ray Sources]

Super-Kamiokande

water tank
1.6 km below ground

50 million liter
ultra-pure water

1 neutrino interaction
every 1.5 hours

neutrino detection
via Cherenkov light

Super-Kamiokande

Super-Kamiokande
Mounting of Photomultiplier Tubes

total number of photomultipliers:

20 inch Ø   11,146

 8 inch Ø   1,885

Super-Kamiokande

SK-I: ^{8}B Solar Neutrino Flux

Super-Kamiokande

Sun

5-20 MeV
[May 31st, 1996 – July 15, 2001]

$$\nu_e + e \rightarrow \nu_e + e \quad \text{[ES]}$$
[comparably high x-sec. due to Z-exchange]

22400 ±230

Event/day/bin

$\cos\Theta_{\text{Sun}}$
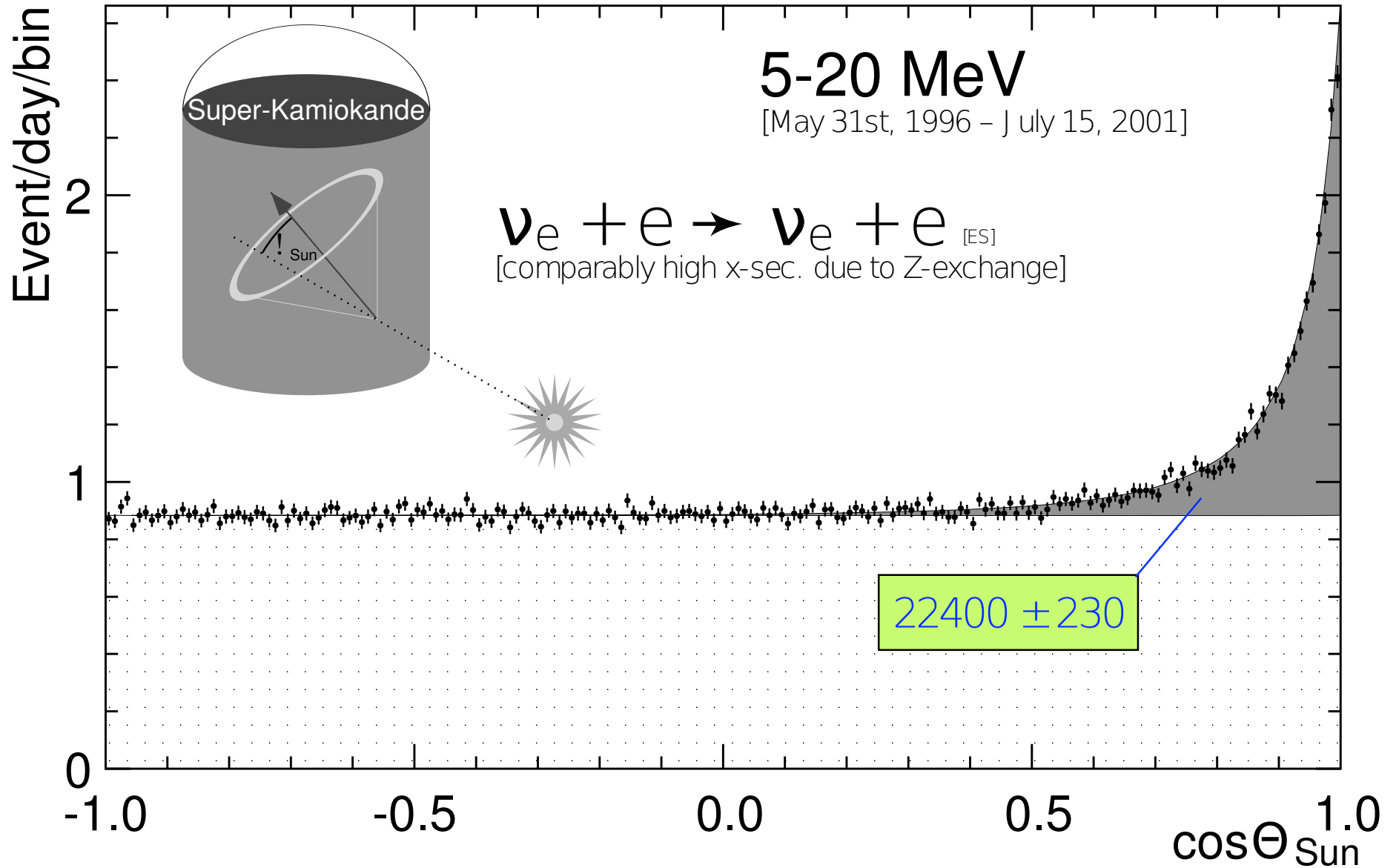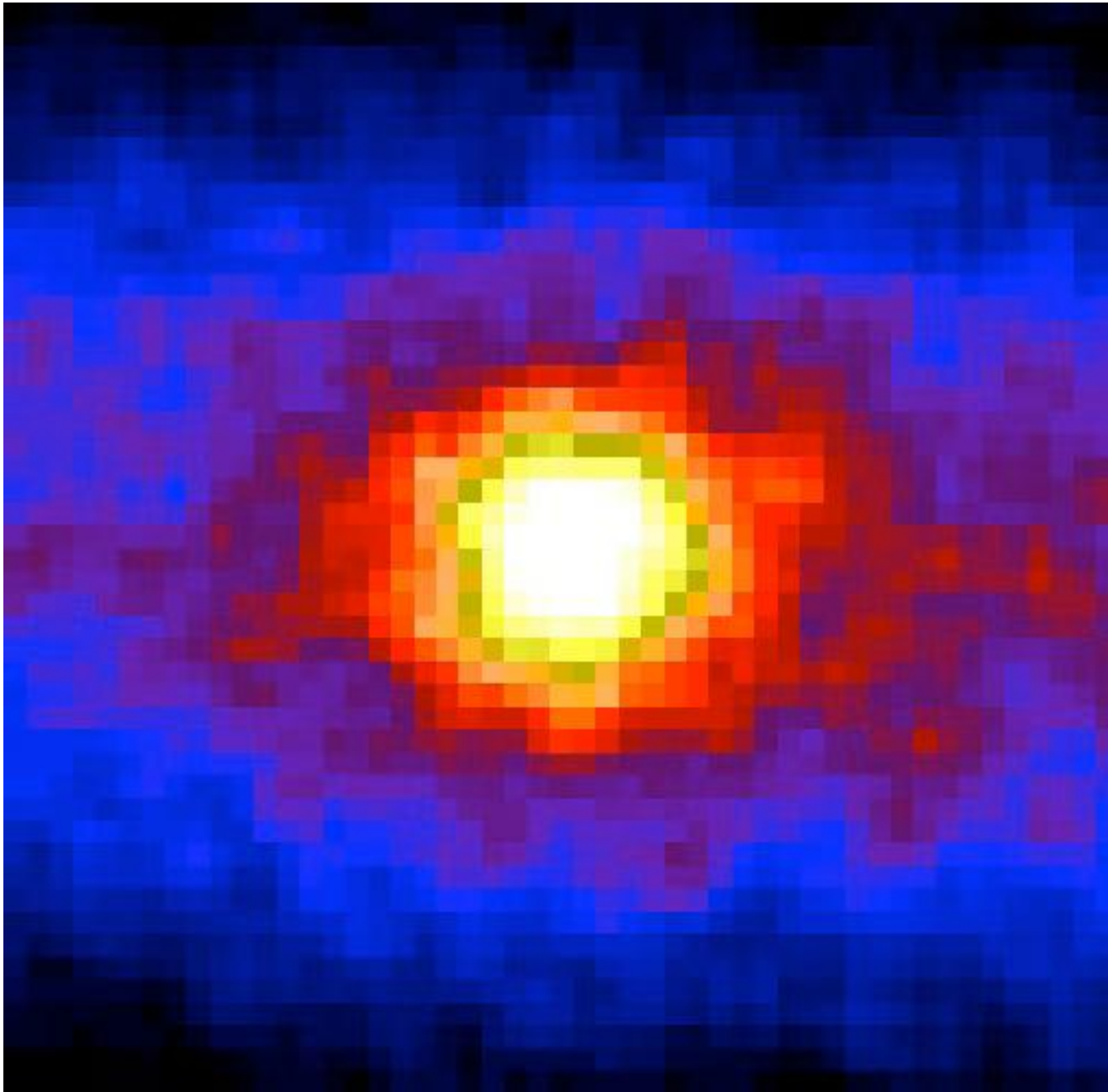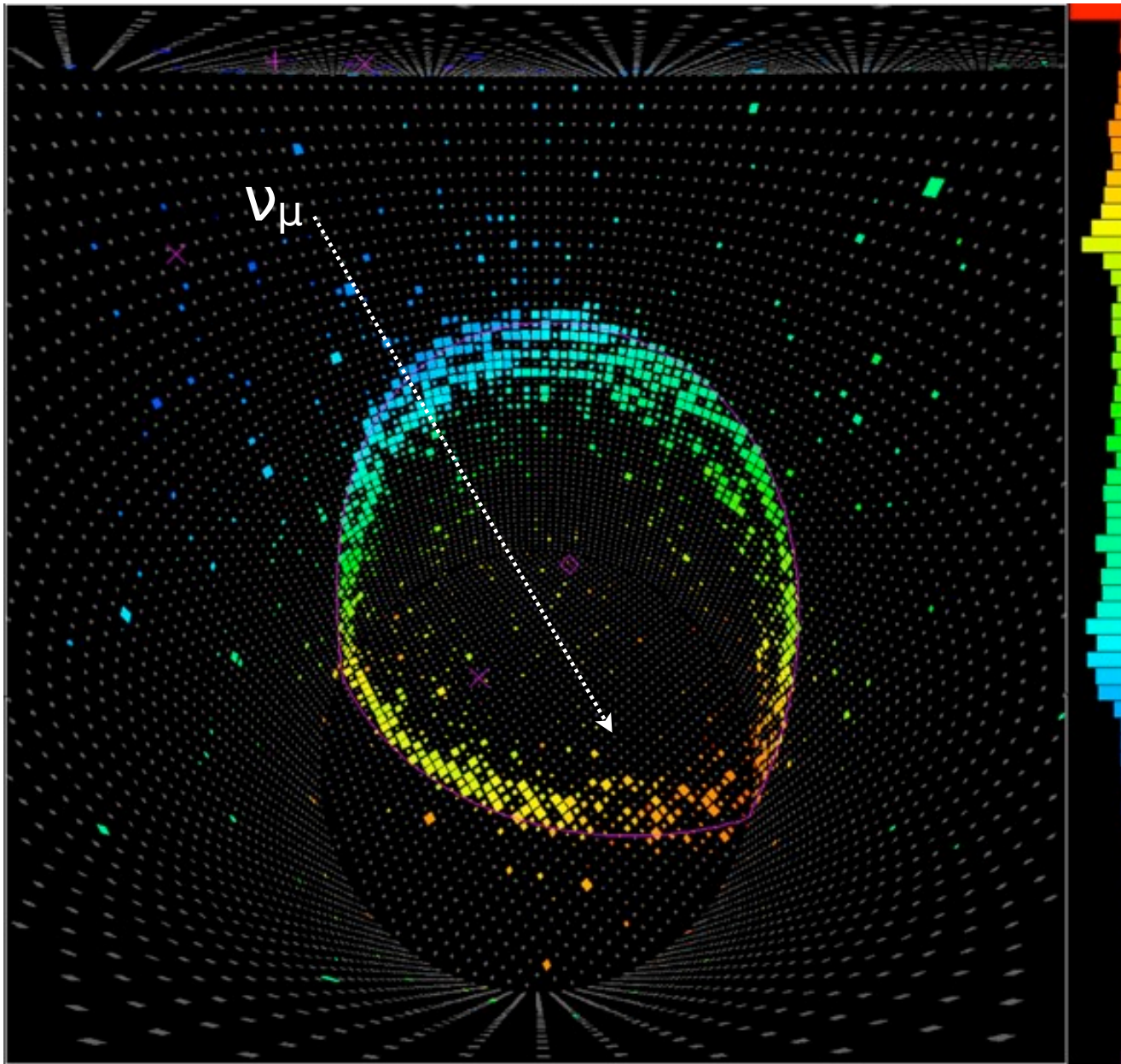
Super-Kamiokande

the sun seen through the earth in neutrino light

Super-Kamiokande

muon event (603 MeV)

observation of clean Cherenkov ring with sharp edges

flight direction from timing measurements
blue: early, red: late

energy from amount of light observed in PMs

Super-Kamiokande

Flight direction
close to view direction
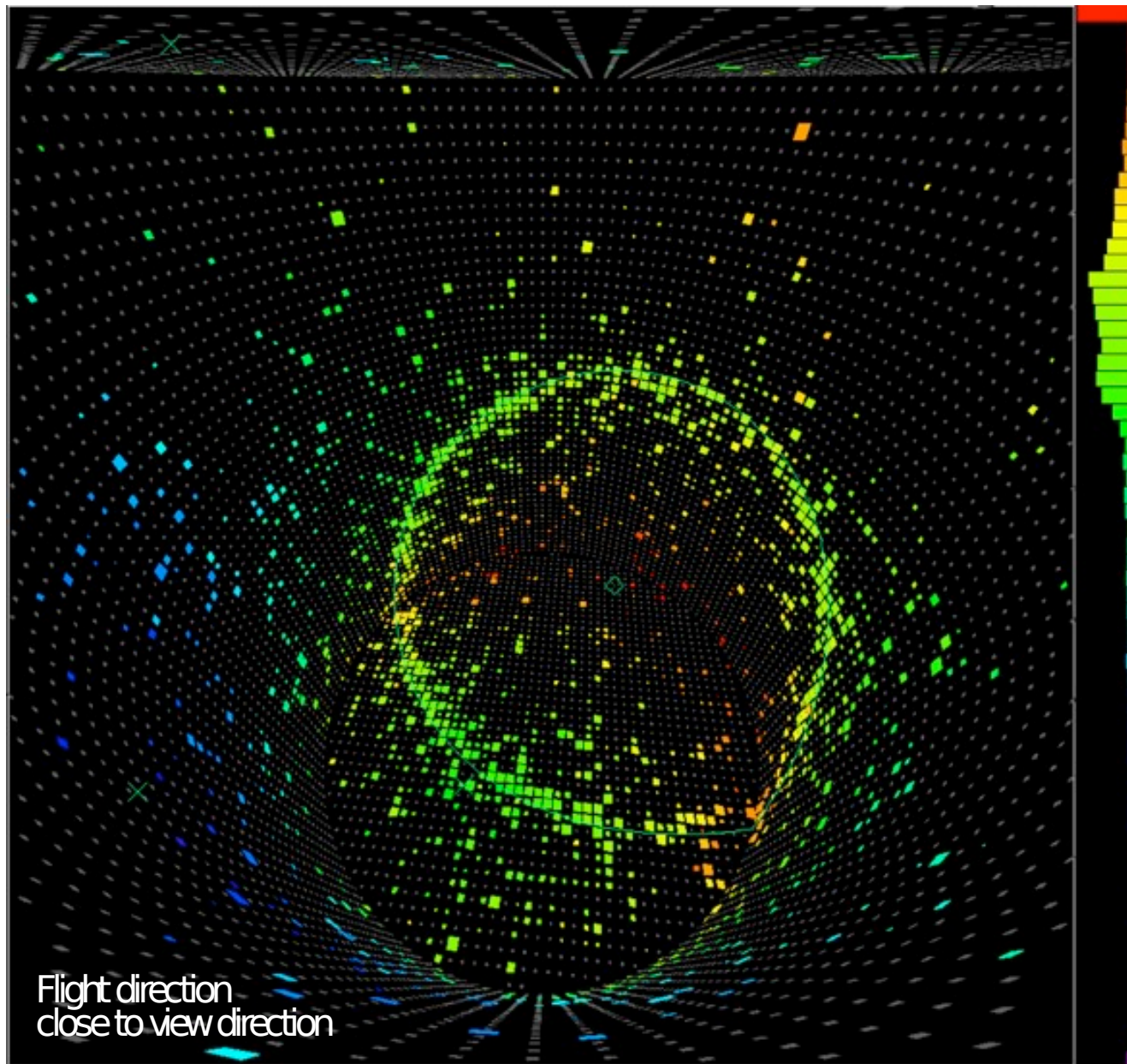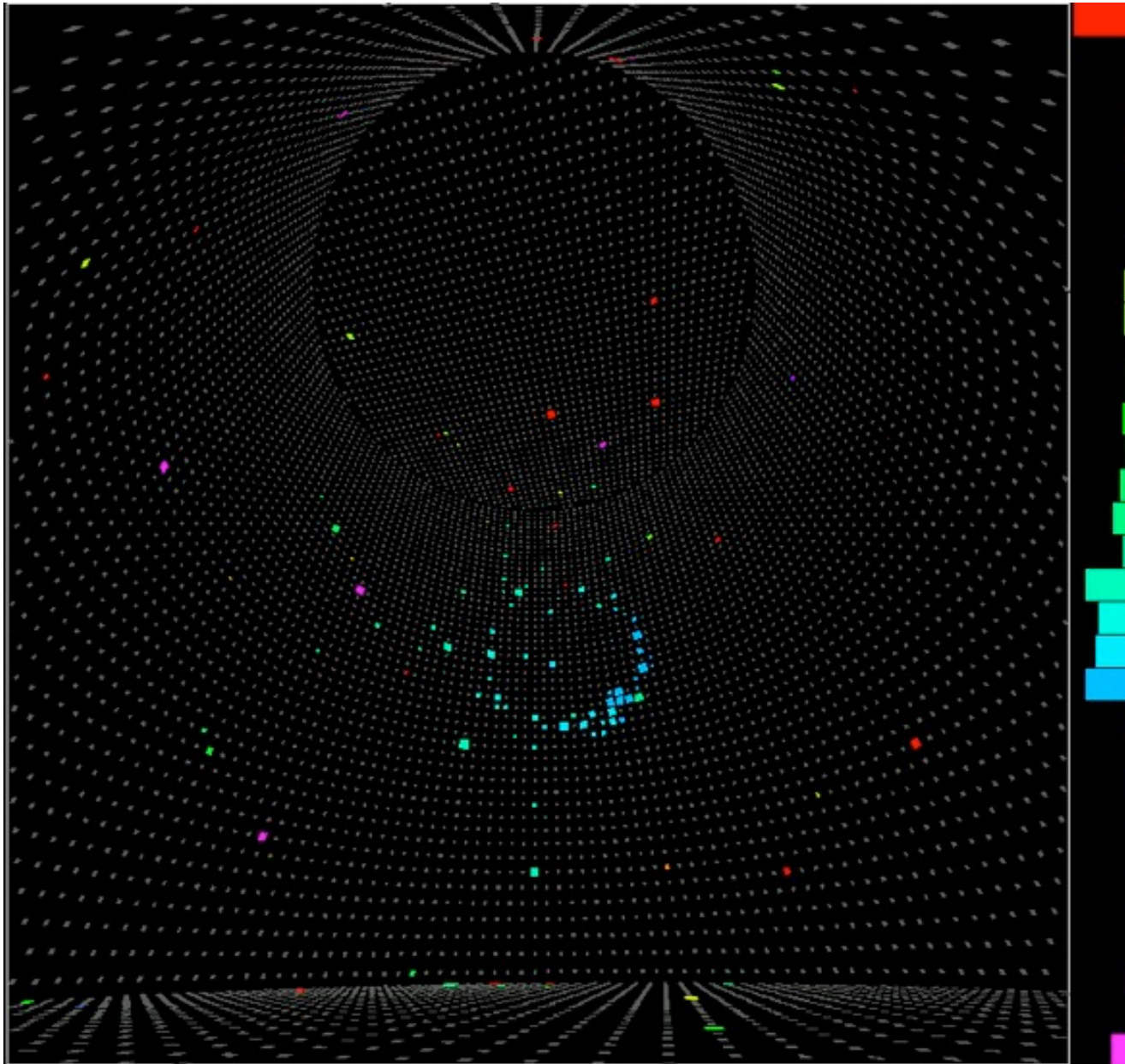
electron event (492 MeV)

observation of Cherenkov ring
with fuzzy edge
(bremsstrahlung)

flight direction from
timing measurements
blue: early; red: late

energy from amount of light
observed in PMs

Super-Kamiokande

solar neutrino (12.5 MeV)

unusually nice, well-defined

flight direction from
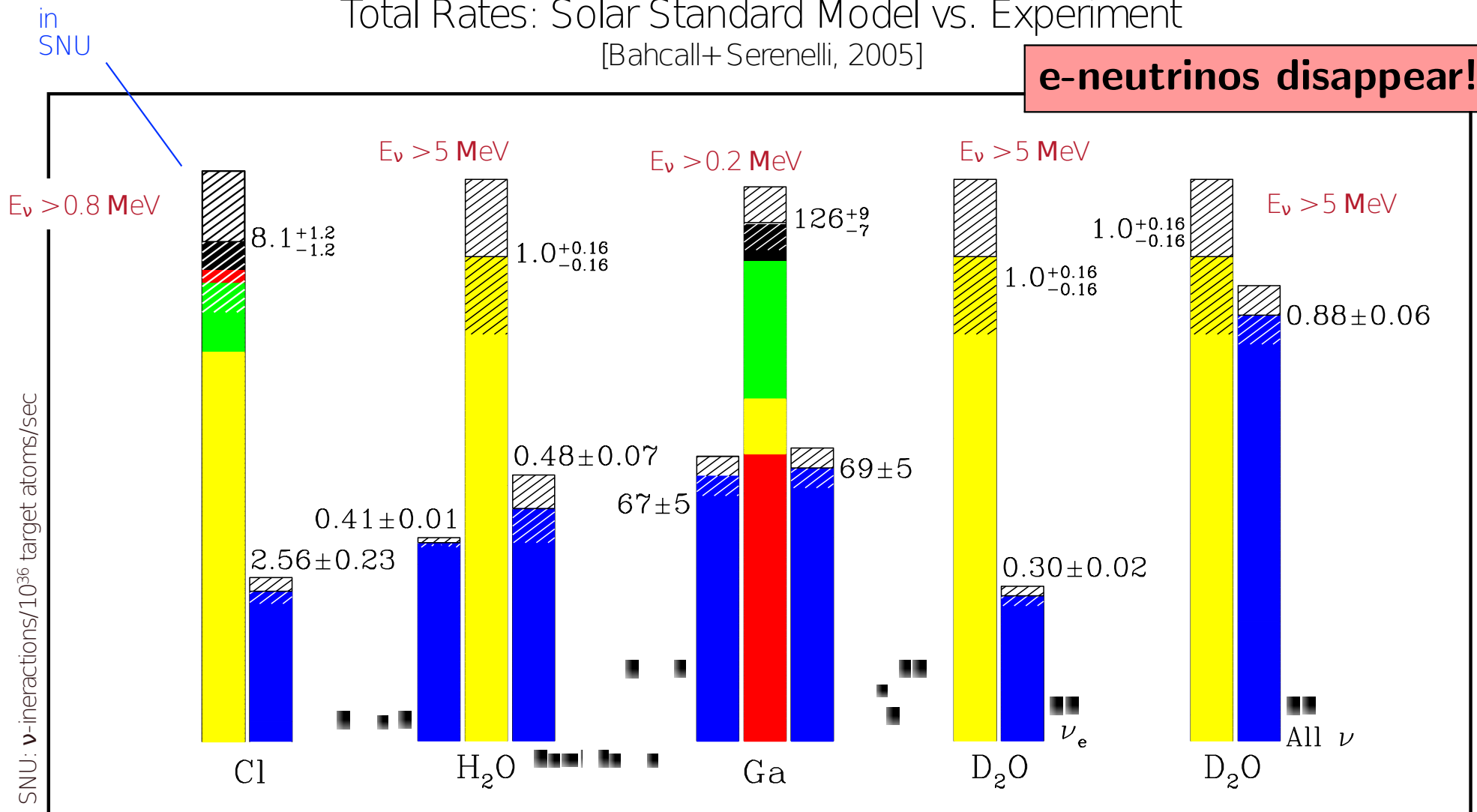timing measurements
blue: early; red: late

energy from amount of light
observed in PMs

Solar Electron-Neutrino Problem

Total Rates: Solar Standard Model vs. Experiment
[Bahcall+Serenelli, 2005]

e-neutrinos disappear!

in SNU

$E_\nu > 0.8$ MeV

$E_\nu > 5$ MeV

$E_\nu > 0.2$ MeV

$E_\nu > 5$ MeV

$E_\nu > 5$ MeV

SNU: ν-ineractions/10^{36} target atoms/sec

$8.1^{+1.2}_{-1.2}$

126^{+9}_{-7}

$1.0^{+0.16}_{-0.16}$

$1.0^{+0.16}_{-0.16}$

$1.0^{+0.16}_{-0.16}$

0.88 ± 0.06

0.48 ± 0.07

0.41 ± 0.01

67 ± 5

69 ± 5

2.56 ± 0.23

0.30 ± 0.02

ν_e

All ν

Cl   H$_2$O   Ga   D$_2$O   D$_2$O

Theory
- ^{7}Be (green)
- ^{8}B (yellow)
- p−p, pep (red)
- CNO (black)

Experiments (blue)
Uncertainties (hatched)

Different Solar Neutrino Experiments

different thresholds
all measure large deficit

- $^{37}Cl \rightarrow {}^{37}Ar$
  (Homestake)

  Exp: 2.6 SNU
  BS05: 8.1 SNU

- $^{37}Ga \rightarrow {}^{37}Ge$
  (Gallex, GNO, Sage)

  Exp: 70 SNU
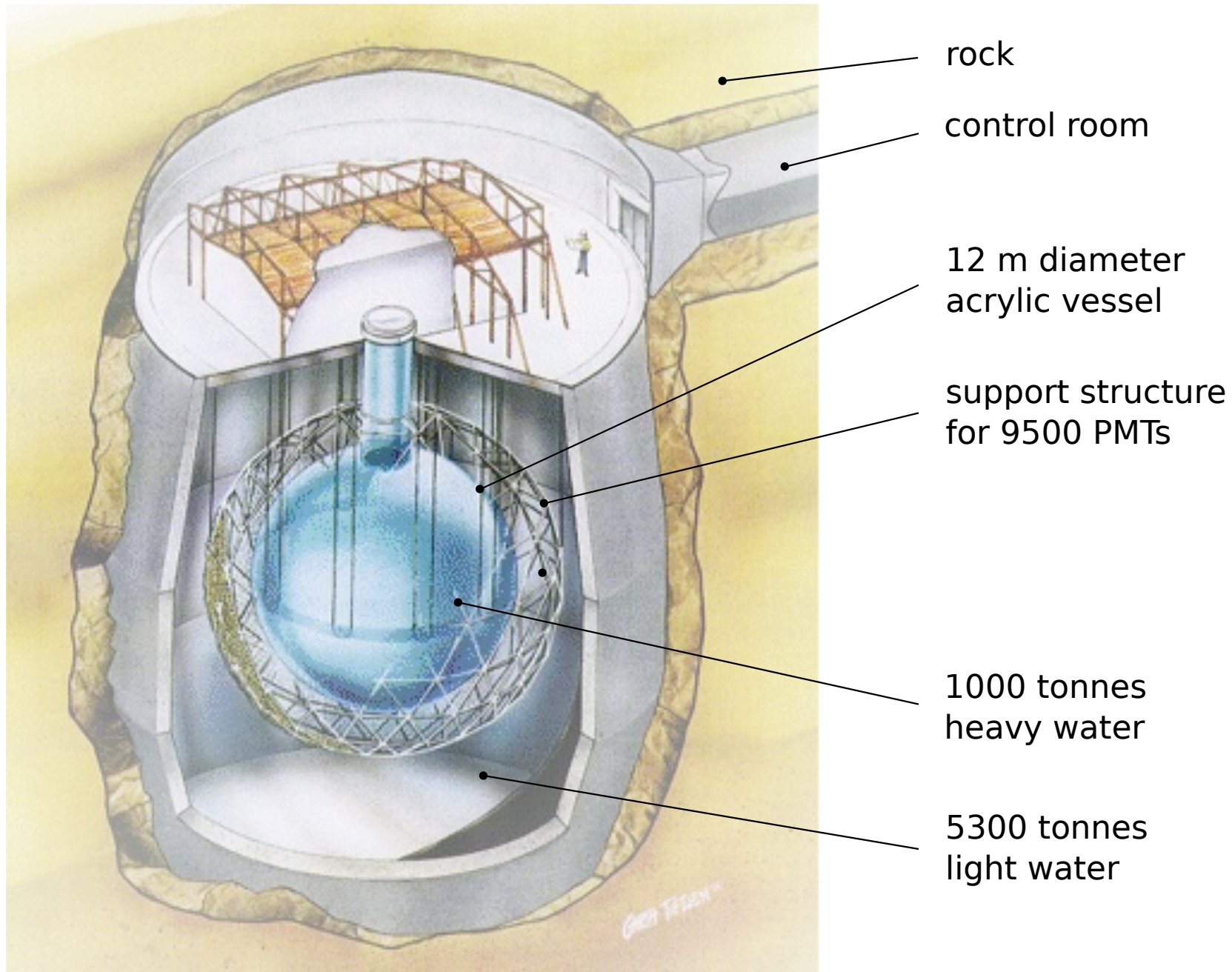 BS05: 126 SNU

- ^{8}B ν_e-flux
  (Kamiokande, SNO)

  Exp: 2.4 SNU
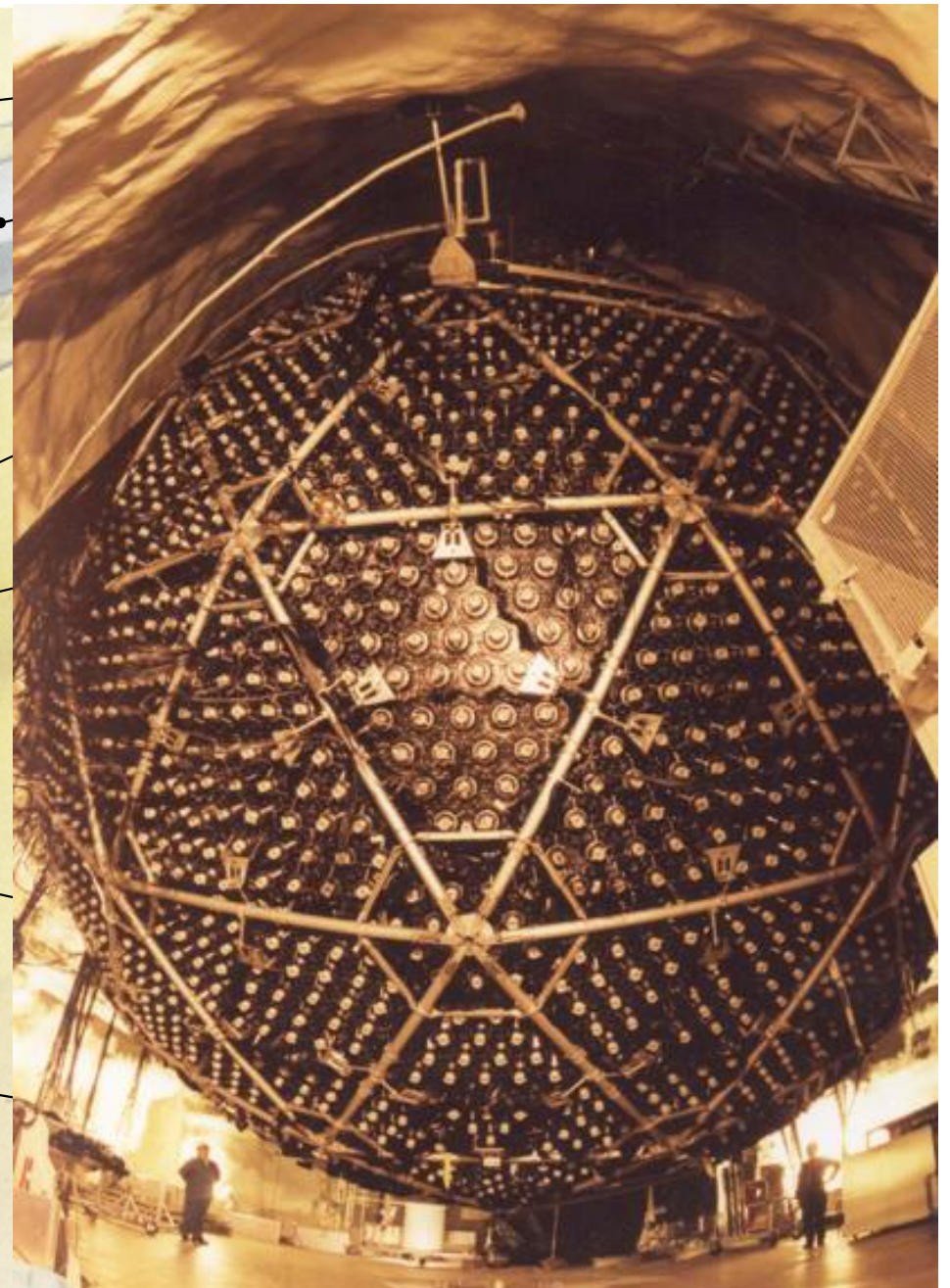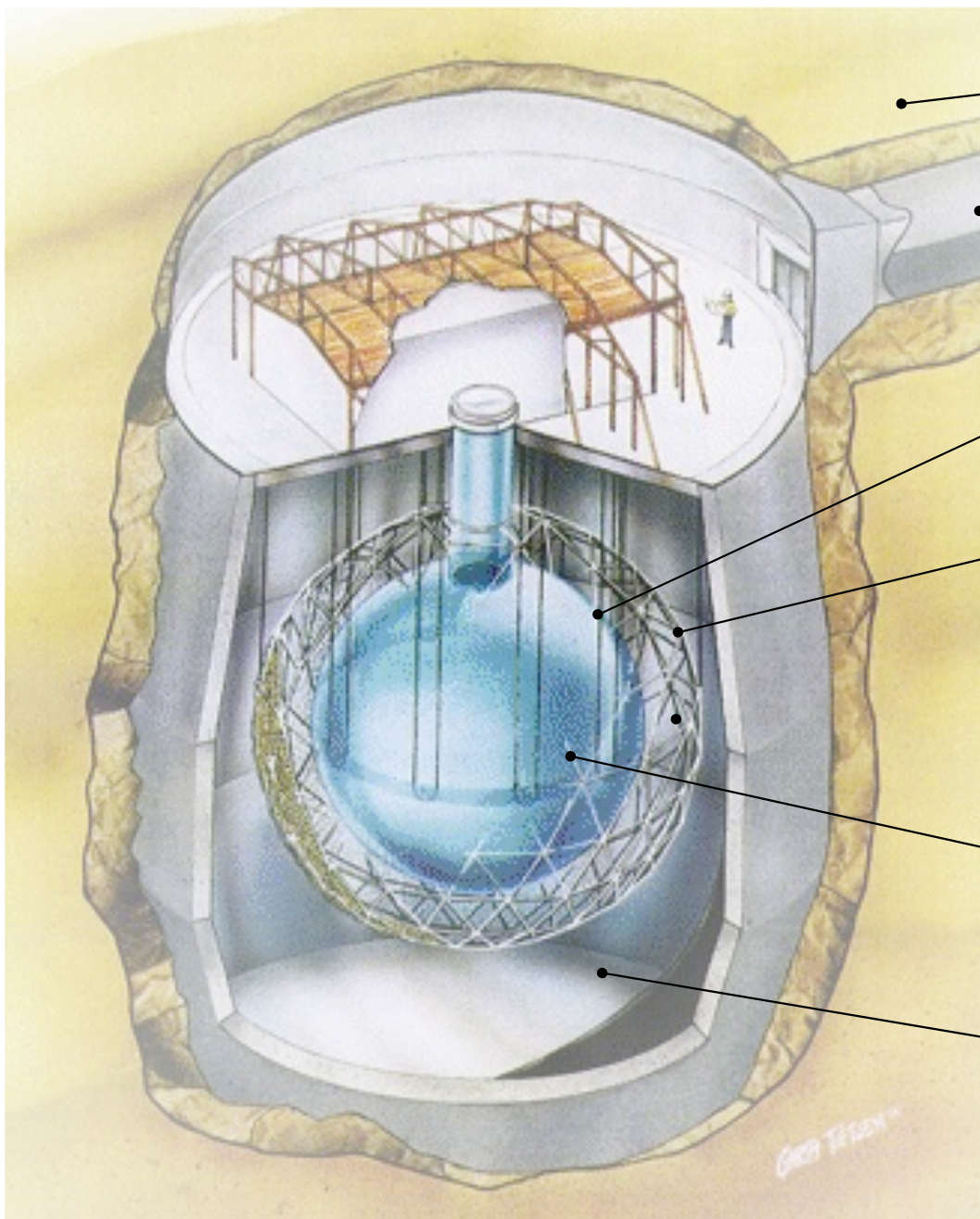 BS05: 5.7 SNU

but SNO has a new twist ... deuterium

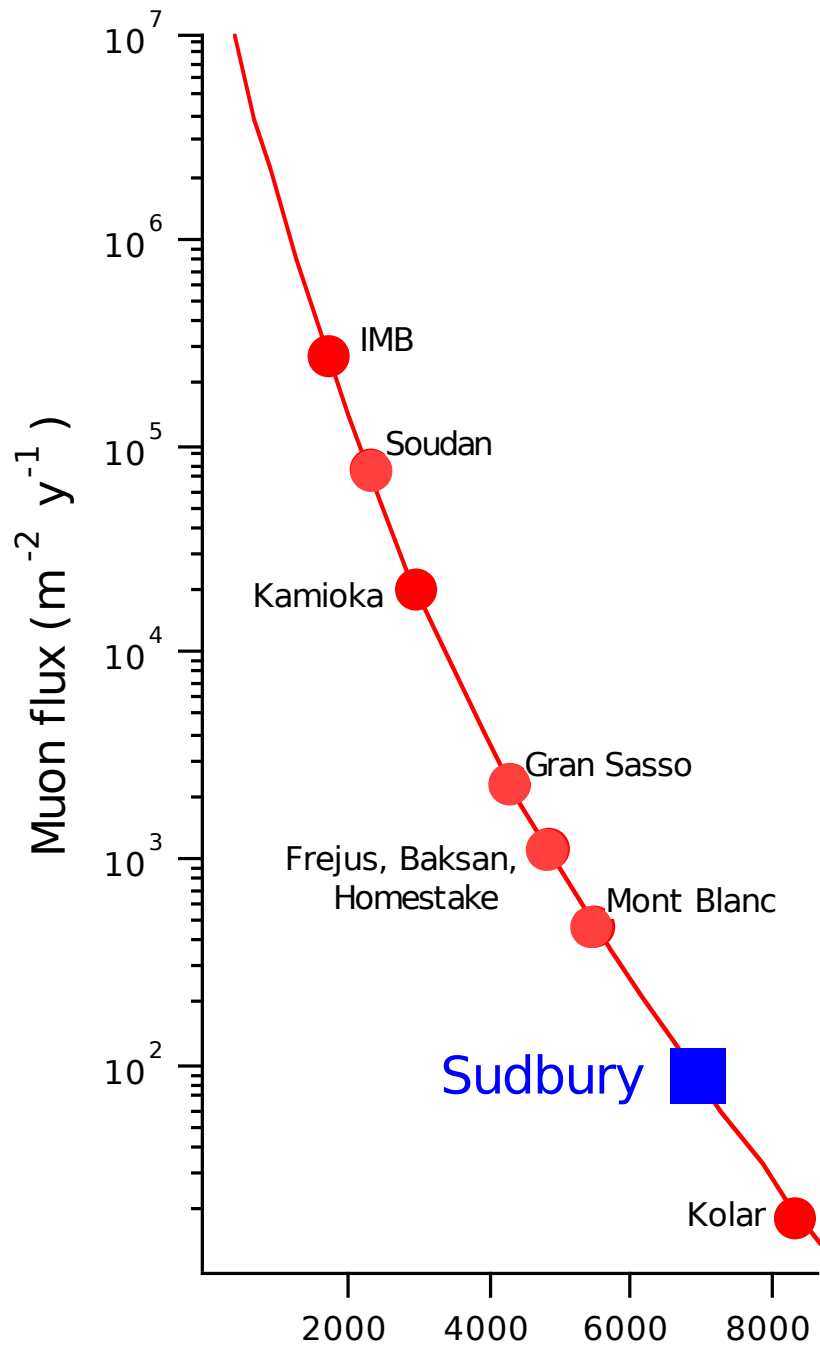|	$^{37}Cl \rightarrow {}^{37}Ar$ (SNU)	$^{71}Ga \rightarrow {}^{71}Ge$ (SNU)	^{8}B ν flux $(10^6 cm^{-2} s^{-1})$
Homestake (CLEVELAND 98)[20]	$2.56 \pm 0.16 \pm 0.16$	—	—
GALLEX (HAMPEL 99)[21]	—	$77.5 \pm 6.2^{+4.3}_{-4.7}$	—
GNO (ALTMANN 05)[22]	—	$62.9^{+5.5}_{-5.3} \pm 2.5$	—
GNO+GALLEX (ALTMANN 05)[22]	—	$69.3 \pm 4.1 \pm 3.6$	—
SAGE (ABDURASHI▷▷02)[23]	—	$70.8^{+5.3+3.7}_{-5.2-3.2}$	—
Kamiokande (FUKUDA 96)[24]	—	—	$2.80 \pm 0.19 \pm 0.33$[†]
Super-Kamiokande (HOSAKA 05)[25]	—	—	$2.35 \pm 0.02 \pm 0.08$[†]
SNO (pure D$_2$O) (AHMAD 02)[4]	—	—	$1.76^{+0.06}_{-0.05} \pm 0.09$[‡]
	—	—	$2.39^{+0.24}_{-0.23} \pm 0.12$[†]
	—	—	$5.09^{+0.44+0.46}_{-0.43-0.43}$[*]
SNO (NaCl in D$_2$O) (AHARMIM 05)[11]	—	—	$1.68 \pm 0.06^{+0.08}_{-0.09}$[‡]
	—	—	$2.35 \pm 0.22 \pm 0.15$[†]
	—	—	$4.94 \pm 0.21^{+0.38}_{-0.34}$[*]
BS05(OP) SSM [13]	8.1 ± 1.3	126 ± 10	$5.69(1.00 \pm 0.16)$
Seismic model [18]	7.64 ± 1.1	123.4 ± 8.2	5.31 ± 0.6

The SNO Experiment

rock

control room

12 m diameter
acrylic vessel

support structure
for 9500 PMTs

1000 tonnes
heavy water

5300 tonnes
light water

The SNO Experiment

The SNO Experiment

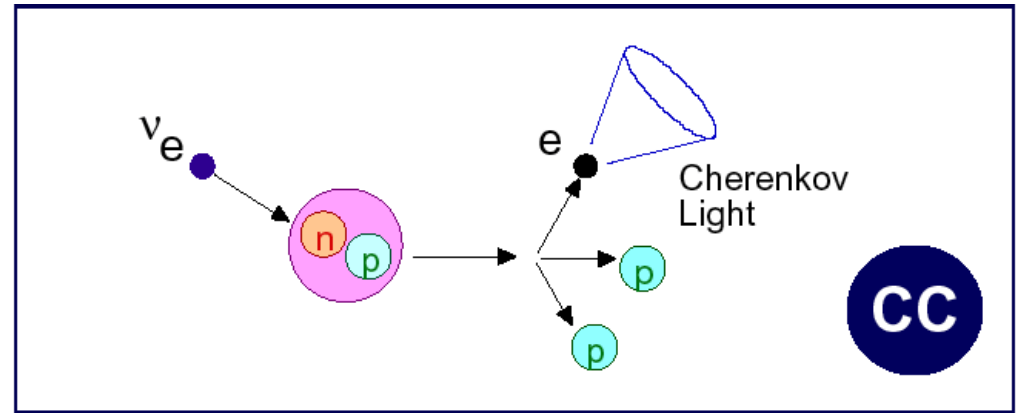
more than 3 km below ground
background < 100 muons/d

The SNO Experiment

charged current

$$\nu_e + d \rightarrow p + p + e^-$$

measurement of ν_e energy spectrum
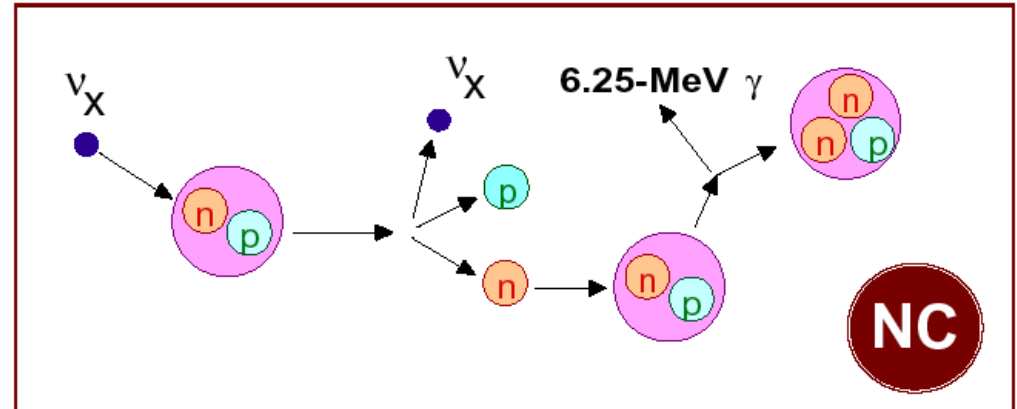weak directionality: $0.34 < \cos\theta < 1$

neutral currents

$$\nu_x + d \rightarrow p + n + \nu_x$$

measure total ^8B neutrino flux from the sun
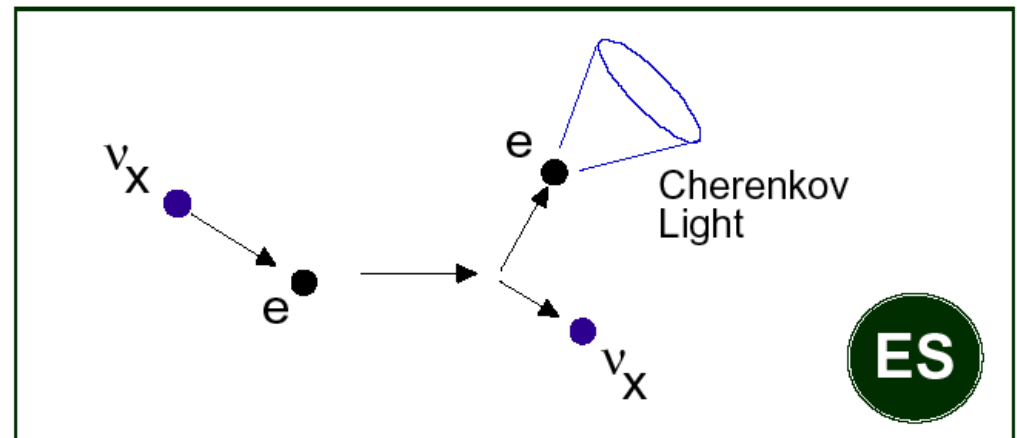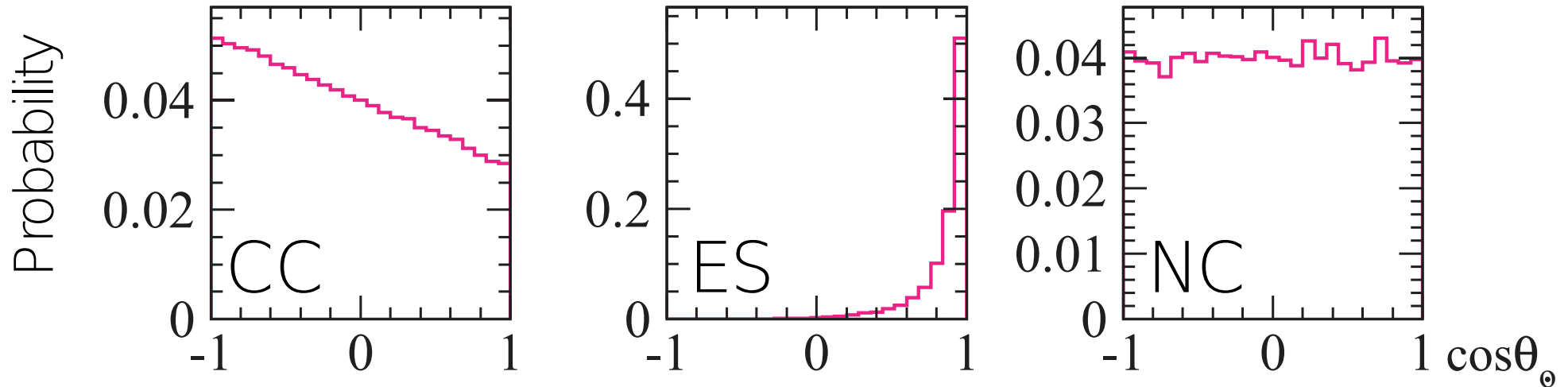$\sigma(\nu_e) = \sigma(\nu_\mu) = \sigma(\nu_\tau)$

electron scattering

$$\nu_x + e^- \rightarrow \nu_x + e^-$$

low statistics
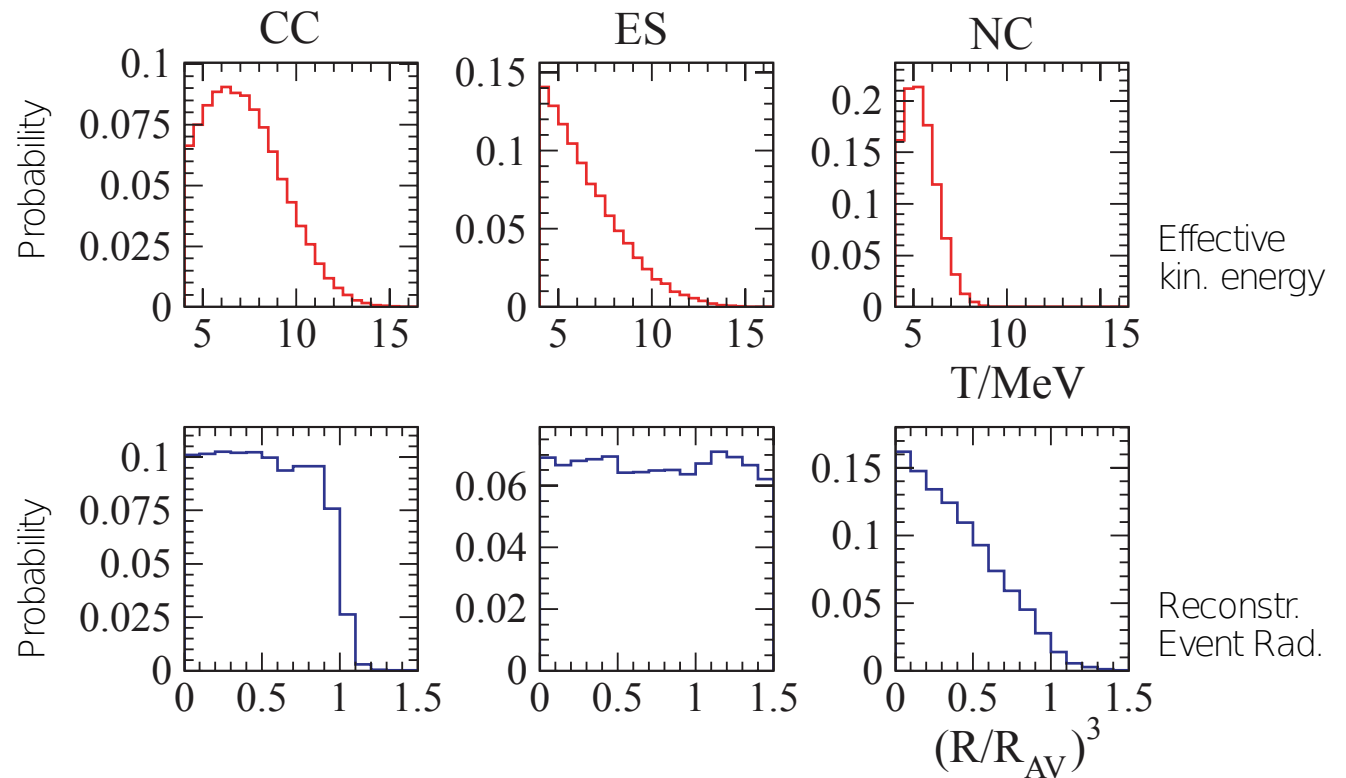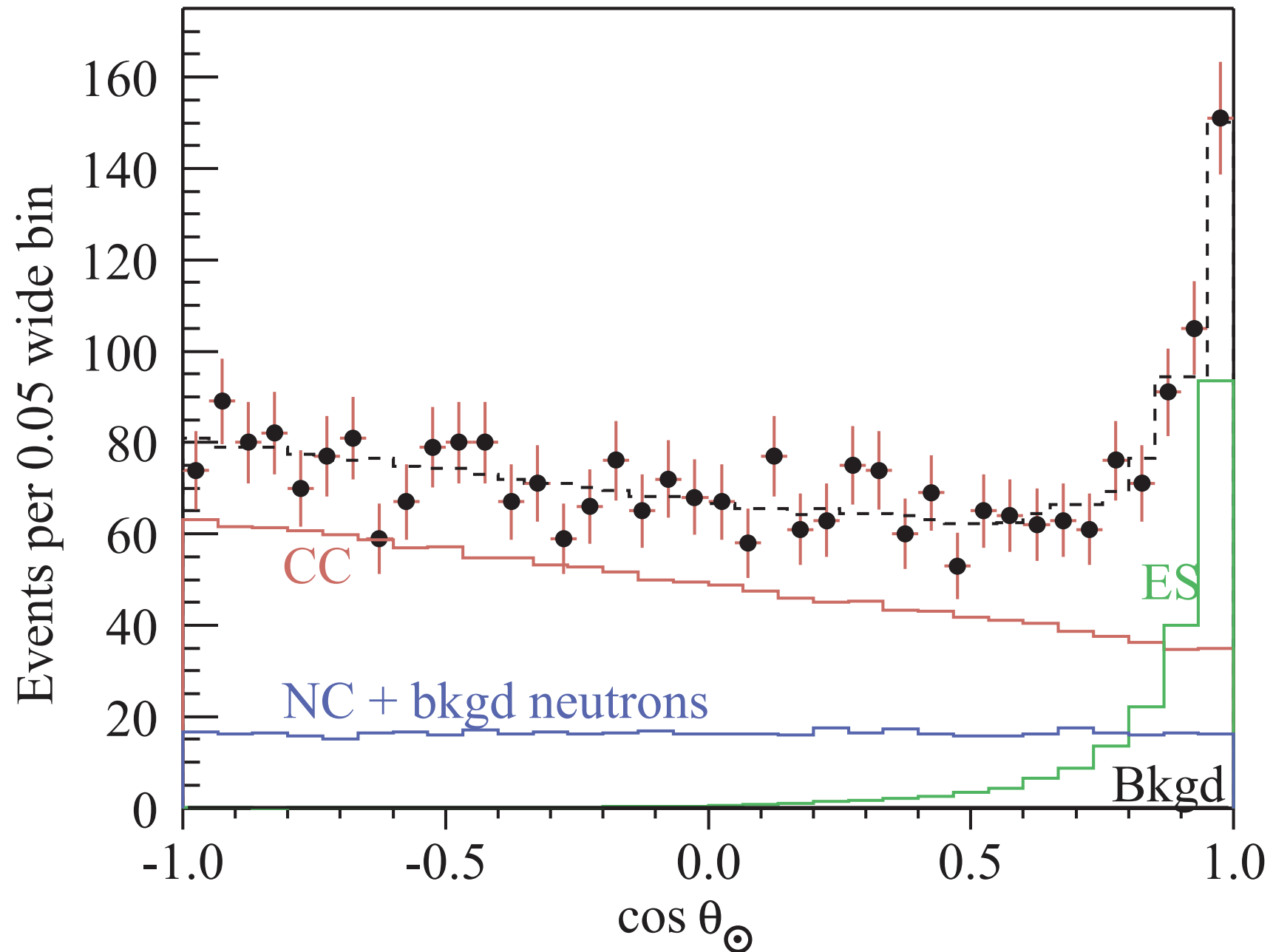strong directionality: $\theta \leq 18°$ ($T_e = 10$ MeV)

The SNO Experiment

analysis strategy:

determine size of
CC, ES, and NC signals
via fit of the data
to probability distributions

The SNO Experiment

The SNO Experiment

$$\Phi_{CC} = 1.76 \; {}^{+0.06}_{-0.05}(\text{stat.}) \; {}^{+0.09}_{-0.09}(\text{syst.}) \cdot 10^6 \; \text{cm}^{-2}\text{s}^{-1}$$

$$\Phi_{ES} = 2.39 \; {}^{+0.24}_{-0.23}(\text{stat.}) \; {}^{+0.12}_{-0.12}(\text{syst.}) \cdot 10^6 \; \text{cm}^{-2}\text{s}^{-1}$$

$$\Phi_{NC} = 5.09 \; {}^{+0.44}_{-0.43}(\text{stat.}) \; {}^{+0.46}_{-0.43}(\text{syst.}) \cdot 10^6 \; \text{cm}^{-2}\text{s}^{-1}$$
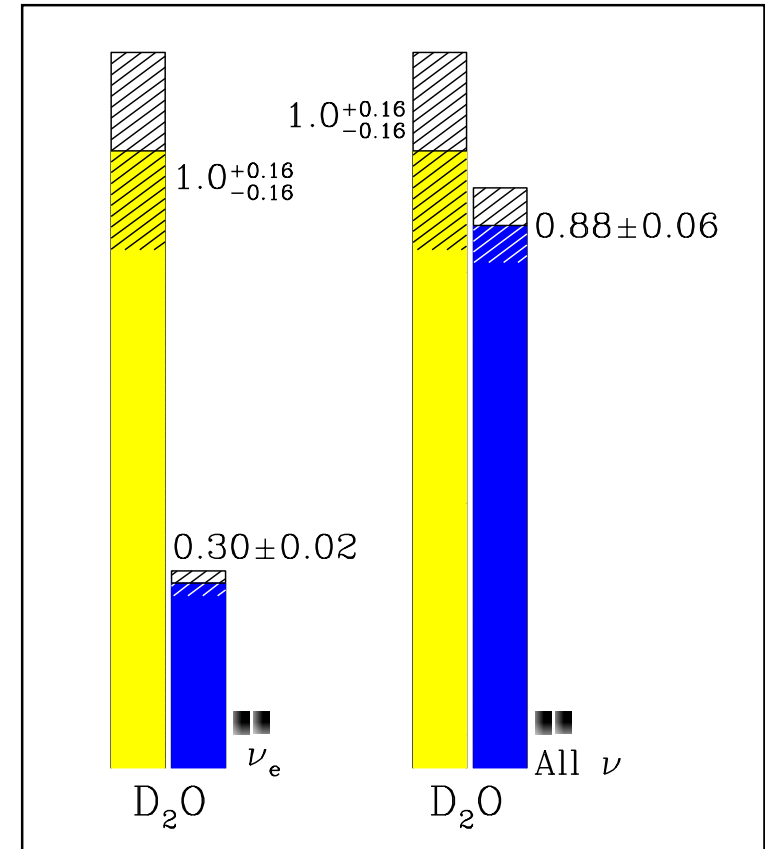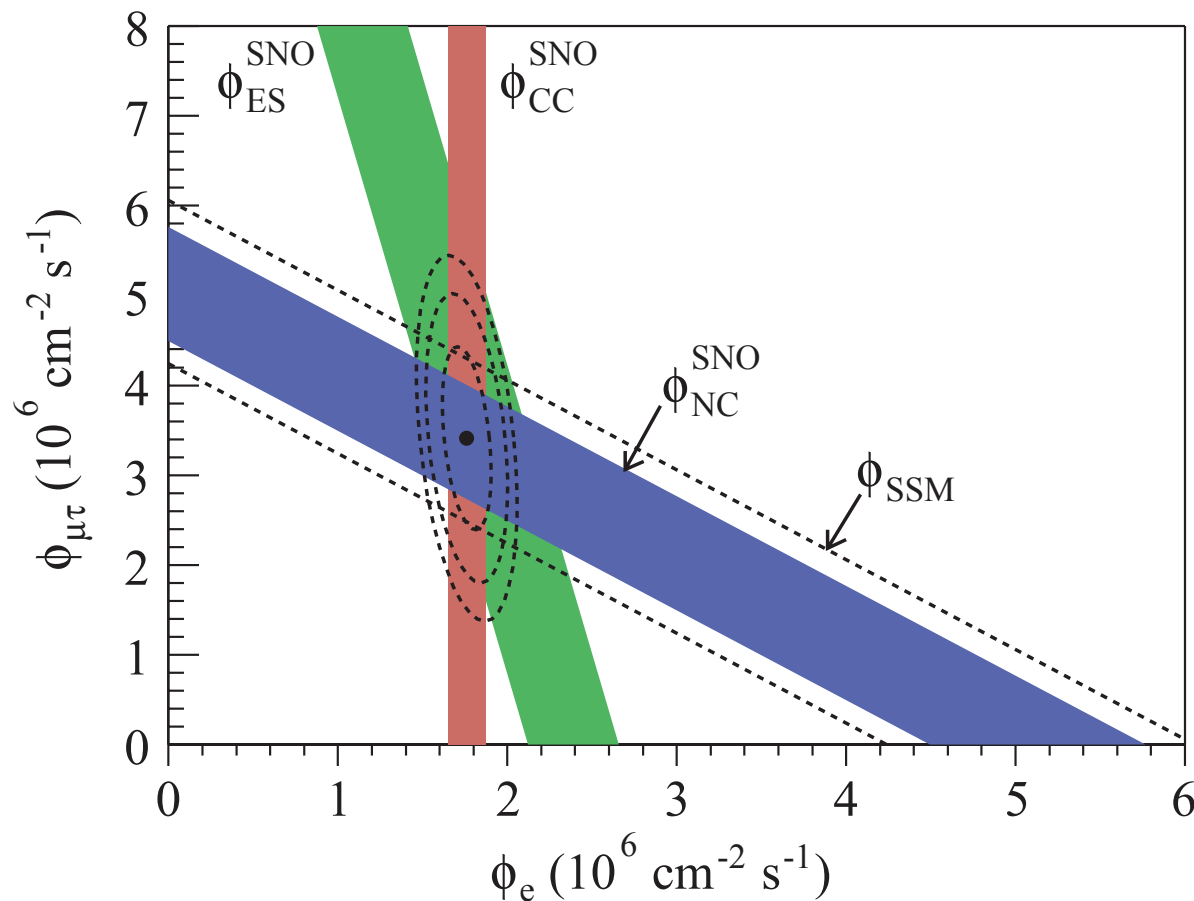
$$\Phi(\nu_e) = 1.76^{+0.05}_{-0.05}(\text{stat.})^{+0.09}_{-0.09}(\text{syst.})$$

$$\Phi(\nu_{\mu\tau}) = 3.41^{+0.45}_{-0.45}(\text{stat.})^{+0.48}_{-0.45}(\text{syst.})$$

$$\cdot 10^6 \; \text{cm}^{-2}\text{s}^{-1}$$

Nobel Prize 2015

Art McDonald - SNO

Takaaki Kajita - Superkamiodande

for the discovery of neutrino oscillations, which shows neutrinos have mass

Cryogenic Detectors

motivation: **WIMP detection**

WIMPs = weakly interacting massive particles

dark matter particles:

must be neutral, i.e. must neither interact via electromagnetic nor strong interactions

WIMPs must be heavy, i.e. non-relativistic (cold dark matter) to allow for galaxy formation

assumed mass range: 10 GeV - 10 TeV

mass limits dependent on cross section, e.g.: $\sigma_{\chi\mathrm{p}} = 1.6 \cdot 10^{-7}$ pb yields $m_{\mathrm{WIMP}} > 60$ GeV

detection via elastic χp-scattering

assume WIMP velocity: $v_\chi \approx 300$ km/s, i.e. $\beta = 10^{-3}$

solar system speed w.r.t. to milky way: $v = 250$ km/s
velocity of earth moving w.r.t solar system: $v = 30$ km/s

maximum energy transfer for collision with nucleus N:

$$T_{\mathrm{N}}^{\max} = 2 \frac{m_\chi^2 M_{\mathrm{N}} c^2}{(m_\chi + M_{\mathrm{N}})^2} \beta^2 \quad (\approx 2 M_{\mathrm{N}} v_\chi^2 \text{ for } m_\chi \ll M_{\mathrm{N}})$$

for e.g. $M_{\mathrm{N}} = 100$ GeV: $T_{\mathrm{N}}^{\max} \approx 100$ keV

Cryogenic Detectors
How to detect WIMPs

transferred energy of recoiling nuclei generally much smaller ($< 10\%$)

need detector that allows detection of recoil nuclei below keV range
energy resolution requires: $n_{\mathrm{excitation}} \gg 1$, i.e. $E_{\mathrm{excitation}} \ll 1$ eV

remember: gases   –   ionzation energy ≈ 30 eV
             silicon   –   electron/hole pair creation ≈ 3 eV

better possibilities:

- phonon excitation:

  maximum phonon energy in Si is 60 meV,
  roughly 2/3 of the energy required for electron-hole formation goes into phonon excitation

- superconducting detectors:

  in superconductors the energy gap 2Δ is equivalent to the band gap in semiconductors
  absorption of energy $> 2\Delta$ (typically 1 meV) can break up a Cooper pair

Cryogenic detectors:

  detect low energies with very good resolution

Cryogenic Detectors

Phonon Detectors

assume thermal equilibrium:

convert absorbed energy into phonons:

$$\Delta T = E/C$$

C: heat capacity of the sample
(specific heat × mass)
E: deposited energy

optimal detector: low heat capacity

example 1: Si-detector at room temperature

$C_{\mathrm{spec}} = 0.7$ J/gK
$E = 1$ keV, $m = 1$ g $\rightarrow \Delta T = 2 \cdot 10^{-16}$ K
not very practical, need lower specific heat and mass

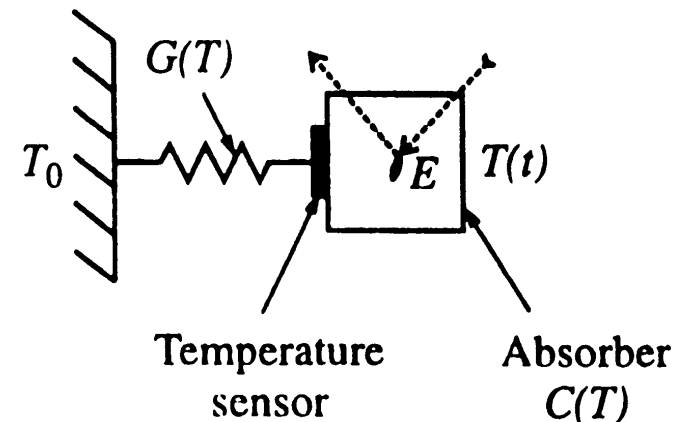example 2: Si-detector at low temperature

$C_{\mathrm{spec}} \propto (T/\Theta)^3$
$C_{\mathrm{spec}} = 2 \cdot 10^{-15}$ J/gK at $T = 0.1$ K
$E = 1$ keV, $m = 15$ μg $\rightarrow \Delta T = 0.04$ K (possible!)

basic configuration of cryogenic calorimeter

resolution:

$$
\begin{aligned}
n &= CT/kT = C/k \\
\sigma_0 &= kT\sqrt{n} = \sqrt{CkT^2} \\
\sigma_E &= \varepsilon\mathrm{Ph}\sqrt{E/\varepsilon Ph} = \sqrt{kTE} \\
\sigma^2 &= \sigma_0^2 + \sigma_E^2
\end{aligned}
$$

yields: $\sigma < 0.2$ eV
(cf. Si semiconductor detector: $\sigma = 20$ eV)

Dark Matter Detection

WIMP

Phonons

Al_2O_3: CRESST-I

" "

T_0 G(T) WIMP

T-sensor

Absorber C(T)

E

Ge, Si: CDMS
Ge: EDELWEISS

$CaWO_4$, Al_2O_3: CRESST

C, F, I, Br:
PICASSO, COUPP
Ge: Texono, CoGeNT
CS_2,CF_4, ^{3}He: DRIFT
DMTPC, MIMAC
$Ar+C_2H_6$: Newage

NaI: DAMA/LIBRA
NaI: ANAIS
CsI: KIMS

LXe: XENON
LXe: LUX
LXe: ZEPLIN
LAr: WARP
LAr: ArDM

LXe: XMASS
LAr, LNe:
DEAP/CLEAN

Charge

Light

conduction band

E_{gap} ! 0.7eV

valence band

Electron semiconductor
energy

conduction band

band
gap electron scintillation
photon

activator
excited states

activator
ground state

valence band

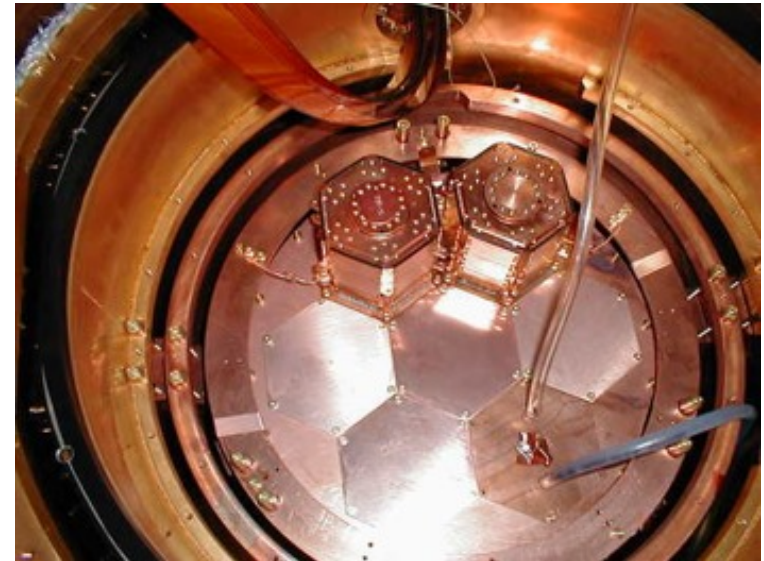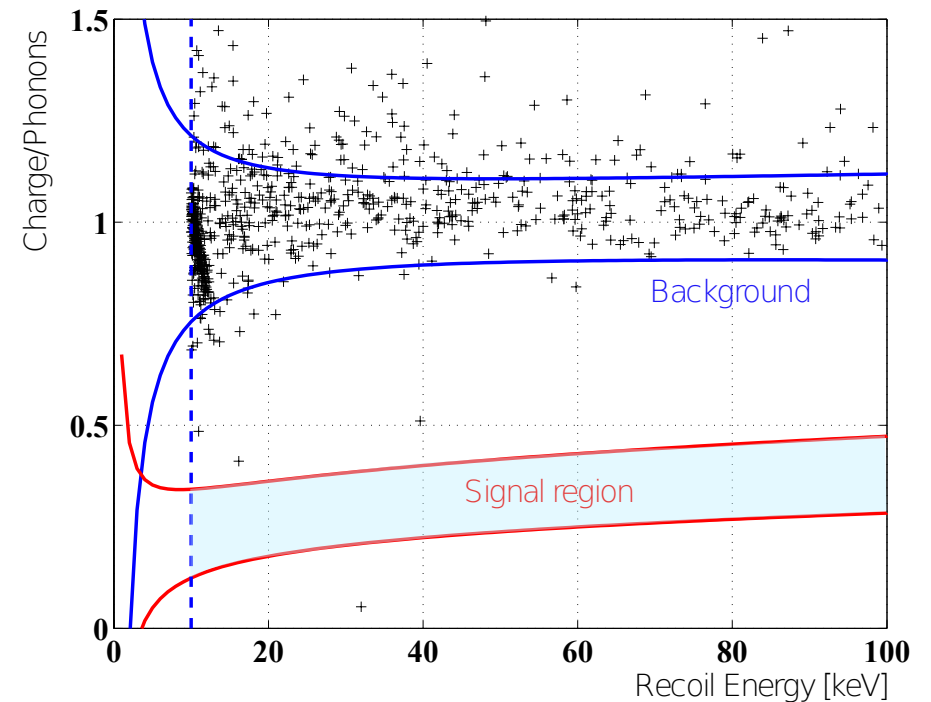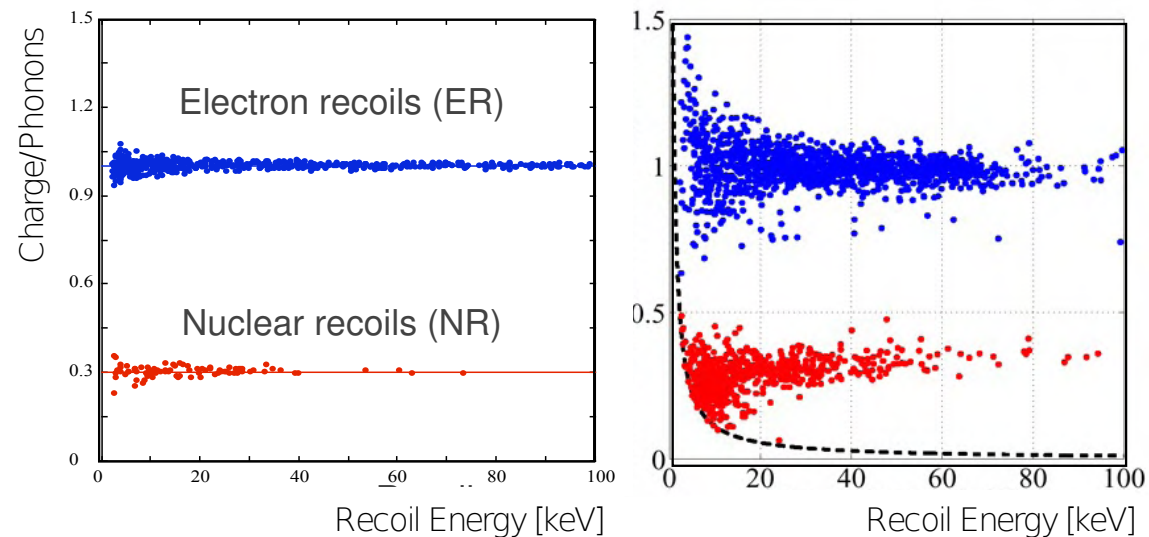# Dark Matter Detection
Example: CDMS

Soudan Underground Lab

5 towers with 6 Ge/Si detectors each operated at $T \approx 20$ mK
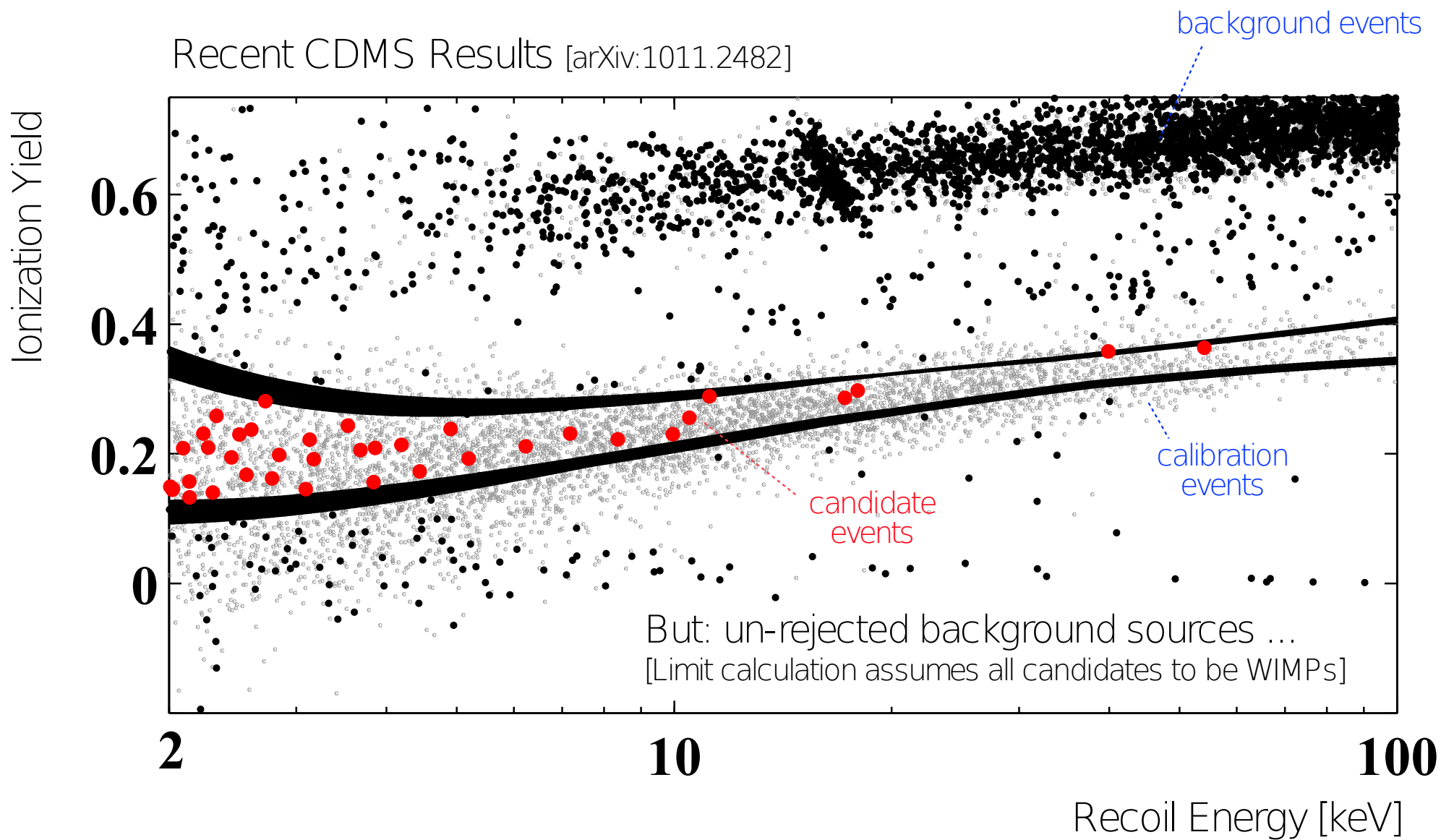
Idea:

WIMPs (and neutrons) scatter off nuclei

most background noise sources (γ,e) scatter off electrons

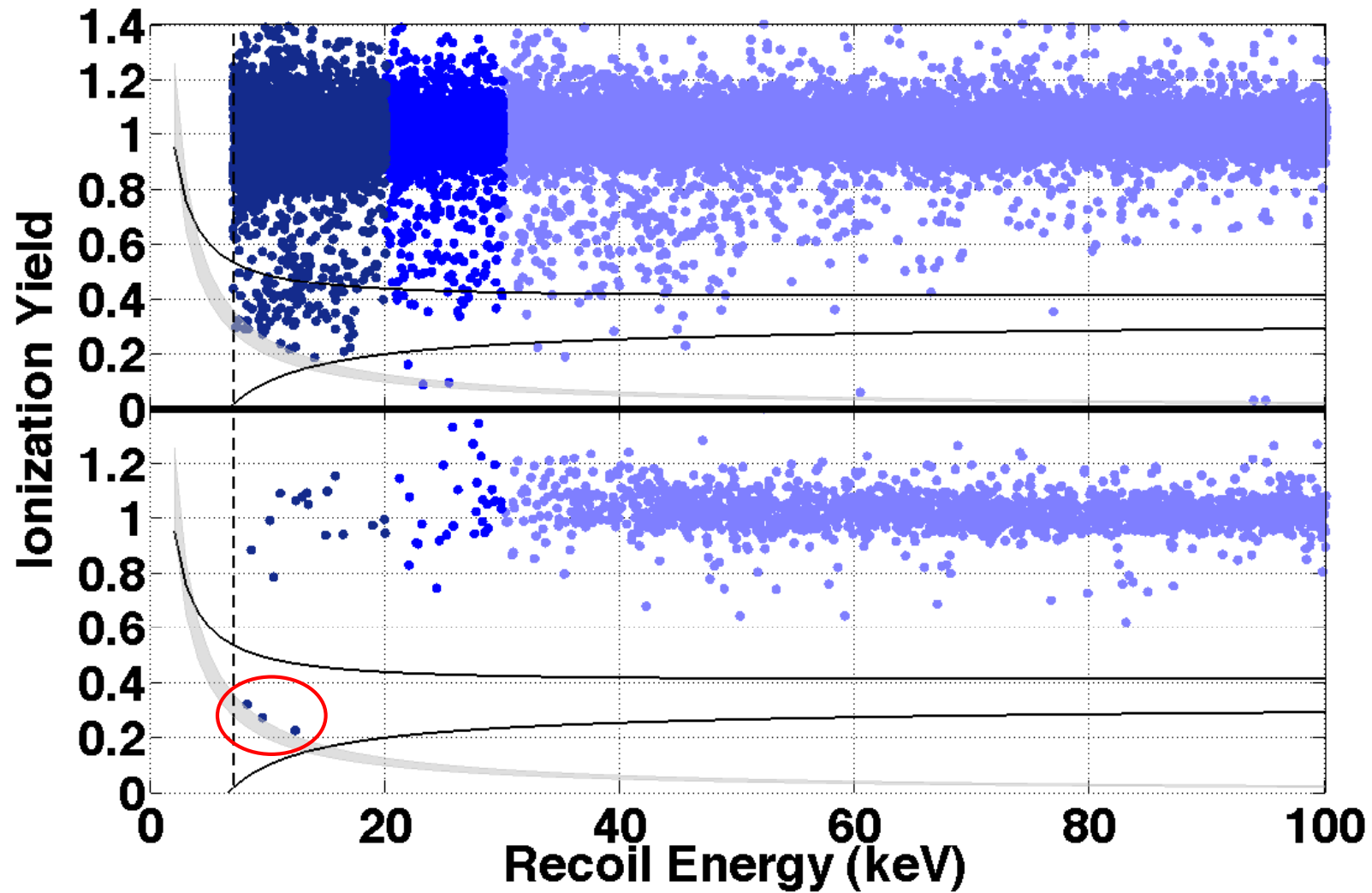ratio ionization/phonons differs for nuclear and electron recoils

Dark Matter Detection

Recent CDMS Results [arXiv:1011.2482]

background events

calibration events

candidate events

But: un-rejected background sources ...
[Limit calculation assumes all candidates to be WIMPs]

Ionization Yield

0.6

0.4

0.2

0

2

10

100

Recoil Energy [keV]

Dark Matter Detection

CDMS II Si 2013 Result

3 candidate WIMPs, 'not yet a discovery'

Dark Matter Detection
Summary Dark Matter WIMP Searches